The Clinical Diagnosis of Porphyrias by Tandem Mass Spectrometry

John Choiniere

A dissertation
submitted in partial fulfillment of the
requirements for the degree of

Doctor of Philosophy

University of Washington

2012

Program authorized to offer degree:
Department of Chemistry

University of Washington

Abstract

The Clinical Diagnosis of
Porphyrias by
Tandem Mass Spectrometry

John R. Choiniere

Chair of the Supervisory Committee:
Professor František Tureček
Department of Chemistry

Heme, a tetrapyrrole ringed molecule essential for life, is synthesized by the body in an eight-step, enzyme-assisted pathway. Each step is catalyzed by an enzyme; a genetic deficiency in any of the last seven of these enzymes is classified as a type of the family of diseases called the porphyrias. Tandem mass spectrometry, which has been previously shown by the Tureček lab to be of use in both newborn screening and in clinical diagnostics, has the potential to be used in the diagnosis of the porphyrias, as the sensitivity and selectivity of the technique can be utilized to develop more efficient and effective assays than those that currently exist.

Here, work towards three new assays is described: an assay for the enzyme 5-aminolevulinic acid dehydratase, deficiency in which causes 5-aminolevulinic acid dehydratase-deficient porphyria (ADP), that utilizes erythrocytes as an enzyme source and detects a butyrated version of the enzymatic product quantified by a deuterated version of the butyrated compound;

an assay for the enzyme ferrochelatase, deficiency in which causes erythropoietic protoporphyria, that utilizes mononuclear blood cells (primarily lymphocytes) as an enzyme source and detects the enzymatic product of two unnatural substrates, cobalt mesoporphyrin IX, quantifying by comparison to cobalt protoporphyrin IX; and an as-yet-incomplete assay for the enzyme uroporphyrinogen III synthase, deficiency in which causes congenital erythropoietic porphyria.

TABLE OF CONTENTS

LIST OF ABBREVIATIONS

5-ALA	5-aminolevulinic acid
ACD	Acid citrate dextrose
ACN	Acetonitrile
ALAD	5-aminolevulinic acid dehydratase
ALAS	5-aminolevulinic acid synthase
but-PBG	Butyrated porphobilinogen
CID	Collision-induced dissociation
CoA	Coenzyme A
COX-2	Cyclooxygenase II enzyme
CPO	Coproporphyrinogen III oxidase
CPO1	Coproporphyrinogen I
CPO3	Coproporphyrinogen III
CYP450	Cytochrome P450 enzyme
DTT	Dithiothreitol
EDTA	Ethylenediaminetetraacetic acid
ESI	Electrospray ionization
GC-MS	Gas chromatography-mass spectrometry
HMB	Hydroxymethylbilane
HPLC	High-performance liquid chromatography
IRB	Institutional review board
LC	Liquid chromatography
MPIX	Mesoporphyrin IX
MPS	Mucopolysaccharidosis
NMR	Nuclear magnetic resonance
ODS	Octadecylsilane
PBG	Porphobilinogen
PBGD	Porphobilinogen deaminase
PPIX	Protoporphyrin IX
PPO	Protoporphyrinogen oxidase
RBC	Red blood cells
RF	Radio frequency
UPLC	Ultra-high-performance liquid chromatography
URO1	Uroporphyrin I
URO3	Uroporphyrin III
UROD	Uroporphyrinogen dehydratase
UROS	Uroporphyrinogen synthase
WBC	White blood cells

LIST OF FIGURES

LIST OF TABLES

DEDICATION

This dissertation is dedicated to my wife, Kate, who struck up a conversation with me over an organic chemistry textbook when we were both undergrads, whom I followed to Washington, and without whom I could not possibly have done this.

Chapter 1
Introduction

1.1 – Mass Spectrometry

Mass spectrometry, to speak broadly, is the measurement of the mass-to-charge (m/z) ratio of an atom or molecule. Though the individual parts can vary quite widely, all mass spectrometers at a basic level consist of the same three parts: an ion source, a mass separator, and an ion detector. Although the theoretical basis dates back to the late 1800s, the field truly began one hundred years ago, with the discoveries of J.J. Thomson (1). Thomson found that an ionized beam of neon sent through magnetic and electric fields will separate into two distinct beams as it bends, based on the mass of the particles in each beam (simultaneously confirming that neon exists as two isotopes). This became the basis for sector mass spectrometers. Additional types of mass analyzers were later developed, such as time-of-flight instruments (where ions are separated by their flight time through a fixed-length tube) (2), ion trap instruments (where ions are contained by electromagnetic fields and sequentially ejected based on their m/z ratios) (3), and a number of others (4, 5), including the quadrupole mass analyzer (6). Many resources exist for further information on the various types; as only a quadrupole was used in the research that will be discussed herein, only that type of instrument will be described further. Similarly, while many varieties of ion sources exist and are in wide use, only electrospray was used in this research, and as such is the only type that will be discussed here.

A quadrupole mass analyzer consists of four metal rods (typically and classically hyperbolic, though other shapes also work) arranged in parallel. Figure 1.1 shows the rod alignment from Wolfgang Paul's original patent application. Voltages are applied to the rods in such a manner

that only ions of a given *m*/*z* will pass through, while others' trajectories will become unstable and will crash before reaching the end (Figure 1.2). Typical operation of a quadrupole either fixes the voltages at precise values, creating a mass filter, or scans the voltages upward so that all ratios in the selected range are given the sequential opportunity to reach the detector. Resolving power depends on the slope of the scan line, as well as the precision of the applied voltages.

A frequent use of the quadrupole mass analyzer is in a tandem-style instrument, known commonly as a tandem quadrupole or triple quadrupole depending on the precise configurations. This consists of two quadrupoles in series with a collision cell in between them; the collision cell is frequently a quadrupole, hexapole, or octopole, but can be anything that guides ions from the exit of the first quadrupole to the entrance of the other. The specific middle component varies instrument to instrument and manufacturer to manufacturer. Common to all versions, however, is that the first and last analyzers have the ability to either scan across all *m*/*z* ratios or stay fixed at one specifically, while the middle analyzer is used as a collision cell. The collision cell is set to RF-only mode, which allows all ions in a wide *m*/*z* range to pass through, and flooded with a neutral gas for the ions to collide with in order to undergo collision-induced dissociation (CID). Typically a noble gas such as helium or argon is used, due to the lack of reactivity and well-understood collisional cross-section (8).

Four modes of analysis are commonly used in tandem quadrupole mass spectrometry: product ion scanning, wherein the first quadropole is set to one specific *m*/*z* ratio while the third scans across its entire range, giving information about what ions are produced from a specific molecule by CID and therefore molecular composition and structure; precursor ion scanning, which is the opposite – the third quadrupole is fixed while the first is scanned, thereby giving information about what molecules in the sample can produce a certain CID product; neutral loss

scanning, in which both quadrupoles are scanned but at a fixed offset, revealing molecules which lose a neutral species with a mass equivalent to the offset; and finally (and most importantly herein) selected reaction monitoring, where both quadrupoles are fixed at a specific *m*/*z* ratio, so that the only detected ions come from a specific precursor that fragmented in a specific way, making it a highly selective technique for detecting specific, known analytes.

Electrospray ionization (ESI), along with laser-desorption ionization, has revolutionized the field of mass spectrometry since it was introduced in the late 1980s. While certainly many people and groups worked on the ideas and preceding technology, and the concept of electrospray itself dates to the 16th century, its invention is typically credited to John Fenn (most notably in the form of the 2002 Nobel Prize in Chemistry) by way of a paper published in 1989 (9). ESI is a soft ionization source, which is to say the molecule being ionized without the breaking of any chemical bonds within the molecule (although some fragmentation can occur in the ion source, depending on the source's specific parameters). Ions most typically occur through the addition of a cation, commonly hydrogen, sodium, or potassium, though the loss of a proton (creating a negative ion) is also known to happen in certain chemical species. Further, unlike the most common ionization methods that predate ESI, it is capable of providing charge states far greater than just a single positive or negative charge. This is especially relevant for large biomolecules, such as proteins and protein fragments, whose *m*/*z* when $z = 1$ is far too large for the operational range of most spectrometers but which are easily handled with increased *z* values.

1.2 – The Porphyrias

One of the most central molecules to life that exists in the human body is a heterocyclic tetrapyrrole molecule known as heme. Four primary types exist in the human body, commonly labeled Heme A, B, C, and O (figure 1.3); others are known as well, but play minor roles (10). The various types are used in a wide variety of ways, typically in conjunction with assorted proteins; the most famous of these is hemoglobin, the oxygen-carrying protein found in blood, but there are many, many others as well. Some examples include:

- Myoglobin, which serves a similar oxygen-carrying and –transporting role as hemoglobin but within muscle tissue.
- Neuroglobin, which also serves to get oxygen to tissue but in the context of the body's nervous system.
- The Cytochrome P450 (CYP450) enzyme family, which accounts for roughly 75% of all human metabolic activity.
- Cytochrome a, b, and c, which are electron-transport membrane proteins (and whose names reflect the particular heme included).
- The peroxidases, including catalase.
- Prostaglandin endoperoxide synthase, better known as COX-2, important in the detection of pain.

The heme prosthetic group in each of these (indeed, all heme) is synthesized from a single base version, heme B (11). For simplicity's sake, from here onward, this will be referred to simply as "heme" (while other versions, if mentioned, will retain their full name). Heme is synthesized in the body in an eight-step, enzyme-assisted pathway (12). While this primarily occurs in the bone marrow and the liver (as the highest-volume uses of heme are

hemoglobin and CYP450), due to the wide variety of heme-containing protein used in the body the synthesis does take place to some degree in nearly every type of non-erythrocyte cell.

The process begins simply with glycine and succinyl CoA, and the rate is controlled through a feedback mechanism whereby the presence of completed heme suppresses the initial step. Four of the enzymes involved occur in the cytosol of the cell while the other four occur in the mitochondrion, creating a need to transport certain intermediate both in and out of the mitochondrion; however, this is done independently from the enzymes in this pathway. Glycine and succinyl CoA are used by the first enzyme in the pathway, 5-aminolevulinic acid synthase, to make 5-aminolevulinic acid (5-ALA), which takes place inside the mitochondrion. The 5-ALA is subsequently excreted into the cytosol. Two molecules of 5-ALA are then combined by 5-aminolevulinic acid dehydratase to make porphobilinogen (PBG), with two water molecules left over. Four PBG molecules are combined, with the exclusion of four ammonia molecules, by the enzyme porphobilinogen deaminase to make the short-lived intermediate hydroxymethylbilane (HMB). HMB can then take one of two pathways; it can self-cyclize to create uroporphyrinogen I (URO1), or it can be taken up by the enzyme uroporphyrinogen synthase to create the biologically-significant isomer uroporphyrinogen III (URO3). This is the only step with meaningful non-enzymatic consumption of an intermediate. Both isomers are acted upon by the subsequent enzyme, uroporphyrinogen decarboxylase, which sequentially strips away the four acetyl groups from the uroporphyrinogens while retaining the four propionyl groups, creating coproporphyrinogen I or III. This is the point at which the isomerism becomes important, as only coproporphyrinogen III is a substrate for the next enzyme, coproporphyrinogen III

oxidase, which is found back inside the mitochondrion and removes two specific carboxyl groups, leaving behind vinylic groups at each location creating protoporphyrinogen IX. The tetrapyrrole ring is then oxidized by the next enzyme, protoporphyrinogen oxidase, resulting in protoporphyrin IX. Lastly, ferrous iron is inserted into the protoporphyrin IX by the final enzyme in the pathway, ferrochelatase, creating the finished heme. The entire pathway can be seen in figure 1.4.

As each enzyme must be created by the body, it is quite possible to be genetically deficient in any of them. A genetic deficiency in 5-aminolevulinic acid synthase is called X-linked sideroblastic anemia (13), and will not be discussed further; deficiency in any of the others, though, is clinically referred to as any one of the various porphyrias.

The first-discovered form of the disease was originally observed in 1874, then fully described in 1911, where Hans Gunther referred to the condition he found as "congenital hematoporphyria"; today, this is better known as congenital erythropoietic porphyria, or Gunther's disease, and is one of the rarer types (14). Since then, seven additional forms of the disease have been found, making eight total for the seven relevant enzyme deficiencies. Two forms of the disease result from deficiency in uroporphyrinogen decarboxylase, and are distinguished by the inheritance pattern (as hence the level of residual activity), while in each other case each deficiency has a unique disease (15). All are inherited conditions; five in an autosomal dominant pattern, the other three autosomal recessive. The various types can be broadly classified based on the location in the body in which the enzyme deficiency is most pronounced (either hepatic, in the liver, or erythropoietic, in the bone marrow) as well as by the primary symptoms (either photosensitivity or neuropathy). Incidence rates, while widely acknowledged to be difficult to measure due to underreporting and misdiagnosis, vary widely

among the different types, from an estimated worldwide occurrence of between one and five in 10,000 for the most common, porphyria cutanea tarda (PCT), to fewer than ten confirmed cases ever for the rarest, 5-aminolevulinic dehydratase-deficient porphyria (ADP) (16). Table 1.1 summarizes many characteristics of each type.

1.3 – Applying Mass Spectrometry to Diagnostics and Screening

Since 1999, there has been a joint effort between the Tureček and Gelb research groups at the University of Washington to expand the worlds of both newborn screening and clinical diagnostics through the introduction of mass spectrometry, focusing on lysosomal storage disorders for screening and porphyrias for diagnostics.

On the screening side, that year Gerber developed a screening procedure for mucopolysaccharidosis (MPS) III type B and GM1 gangliosidosis, which result from a deficiency in N-acetyl-α-glucosaminidase and β-galactosidase, respectively (17). Gerber went on to create screening assays for all four MPS III types (A-D) (18, 19). The next advancements were made by Zhou, who developed assays to measure the activities of the enzymes associated with Niemann-Pick and Krabbe diseases (20). Li continued the work, and in 2004 developed a multiplexed assay wherein five separate diseases (Fabry, Gaucher, Niemann-Pick, Krabbe, and Pompe) could be screened for simultaneously from a single sample (21). Li also introduced dried blood spots as a viable biological sample, rather than the fibroblasts used by earlier methods. This allowed for a wider potential application of the screening methods, as dried blood spots are routinely collected from newborns. Wang then furthered the screening effort by developing assays for MPS I and MPS II (22, 23). Blanchard continued the work in 2008 by creating new and better substrates for MPS I, and

her work was adapted by Wolfe to develop a new substrate for MPS II (24, 25). Duffey and Khaliq created assays in 2011 for MPS VI and IV(A) (26-28); Wolfe continued work on improvements to the MPS II assay, as well as to the original MPS III assays, and attempted (though unsuccessfully) to adapt the method for use in diagnosing or screening for metachromatic leukodystrophy (MLD) (29). Most recently, Spacil adapted the existing assays to create a UPLC-MS/MS method to screen for nine diseases simultaneously in a two-minute run. Selected assays from the lab are now in use in newborn screening labs in New York state and Washington state (30-32, 28).

Common to nearly all diseases addressed by the screening assays is the ability to retard the progress of, or potentially even reverse the course of, the diseases if they are diagnosed early enough, hence the incentive to screen for them. On the diagnostics side, such a requirement doesn't exist. As stated before, the focus has been on the porphyrias, which have traditionally been difficult to specifically diagnose and have gone underdiagnosed in general, but which are somewhat treatable once found. In 2008, Wang published his assays for three enzymes in the heme biosynthetic pathway: uroporphyrinogen decarboxylase (whose deficiency causes either porphyria cutanea tarda or hepatoerythropoietic porphyria), coproporphyrinogen III oxidase (hereditary coproporphyria), and porphobilinogen deaminase (acute intermittent porphyria) (33, 34). In each case, an appropriate and accessible sample is used (either erythrocytes or lymphocytes, depending on the enzyme in question) and is fed a substrate known to work with the enzyme under analysis; the enzymatic product is then quantified by tandem mass spectrometry.

In both the screening and the diagnostic tracks of this project, tandem mass spectrometry is used as the detection method of choice. Specifically, the mass spectrometer is used in the

selected reaction monitoring mode described before. This allows for highly precise detection of the analytes of interest, making the assays very specific and selective. This specificity and selectivity, then, allows for the multiplexed analysis of many assay products at once, since the overlap of both precursor and product ion masses between two assays is extremely unlikely, and can be avoided if necessary through substrate design.

The work described herein furthers the diagnostics project through the development of assays for two additional forms of porphyria. In the first section, a completed assay for ADP (also called Doss porphyria, after its discoverer) will be described. In the second, a completed assay for erythropoietic protoporphyria, or a deficiency in ferrochelatase, will be described. Lastly, work towards an assay for congenital erythropoietic porphyria will be briefly discussed, as well as a significant obstacle to the complete development of a mass spectrometry-based method.

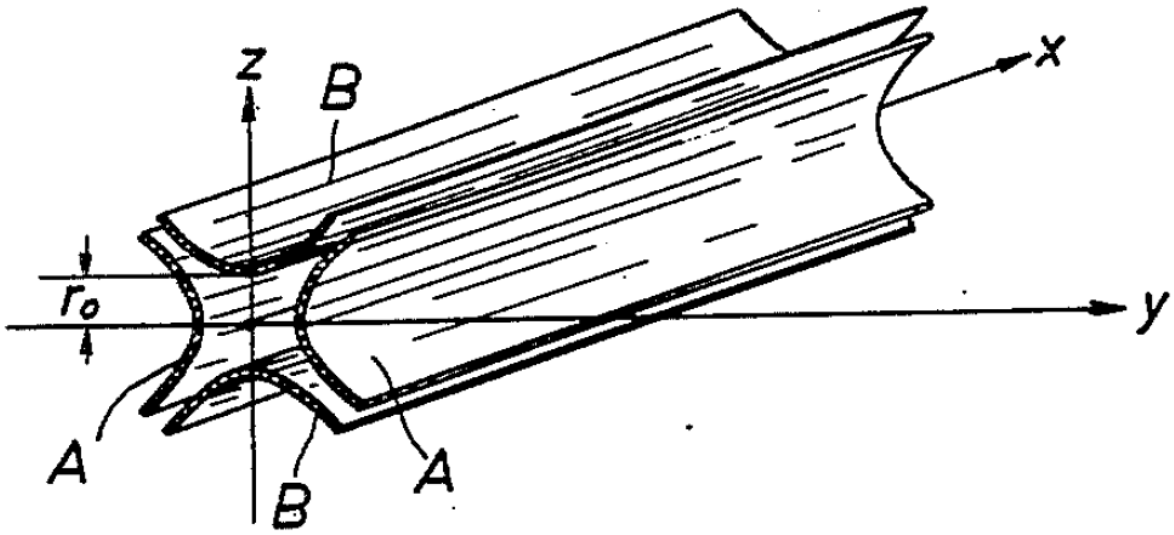

Figure 1.1. Schematic view of the alignment of four hyperbolic rods (shown hollowed out for clarity) in a quadrupole mass analyzer. From the original patent application by Wolfgang Paul (6).

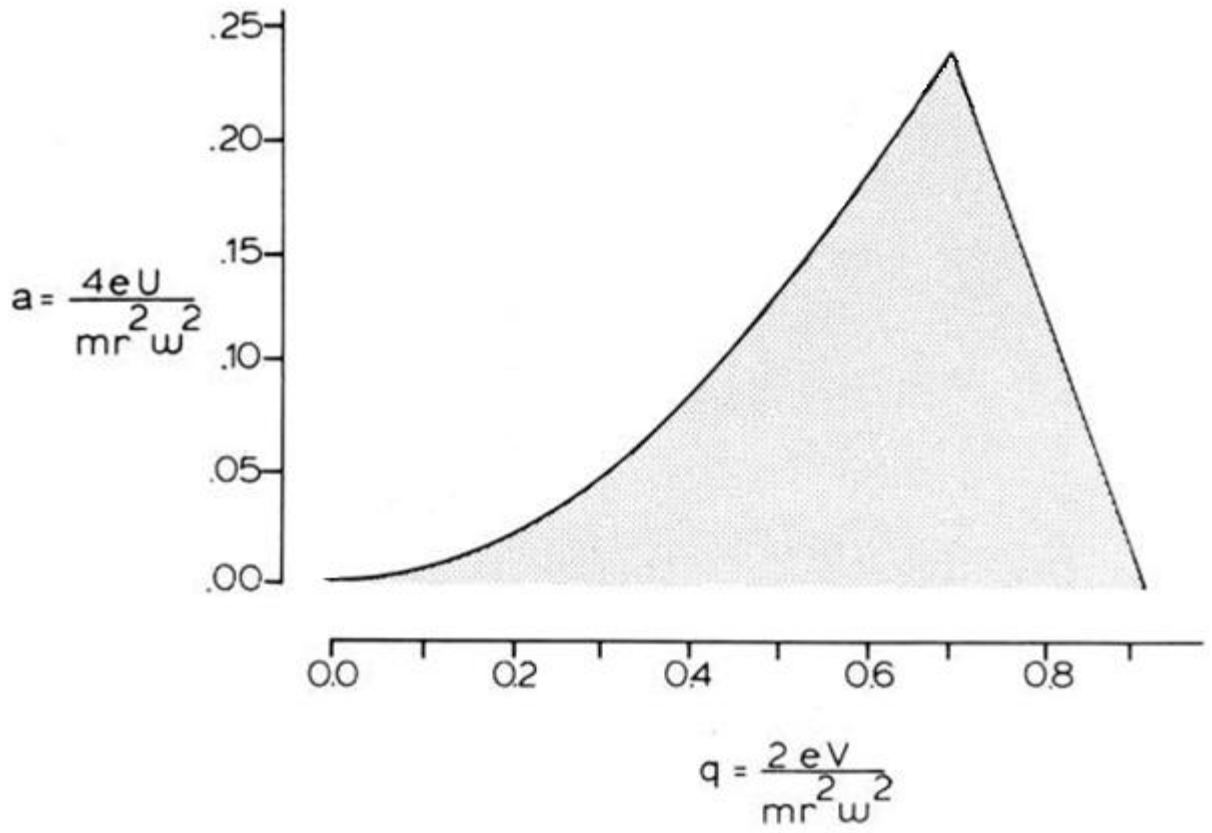

Figure 1.2. Quadrupole mass analyzer stability diagram, in (*a*,*q*) space. Mass-to-charge ratio (or, more accurately, charge-over-mass) affects both parameters (seen in the equations as "e" and "m" respectively); U is the DC voltage applied, and V is the RF. Adapted from Miller and Denton (7).

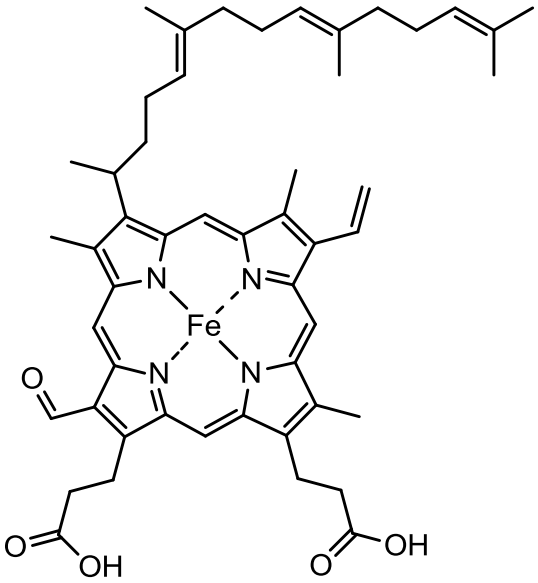

Heme A

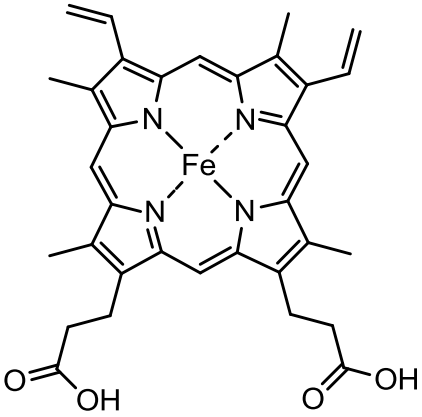

Heme B

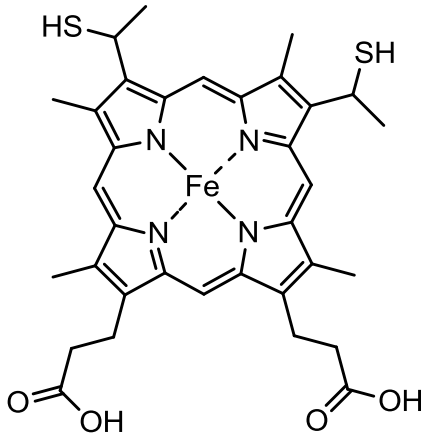

Heme C

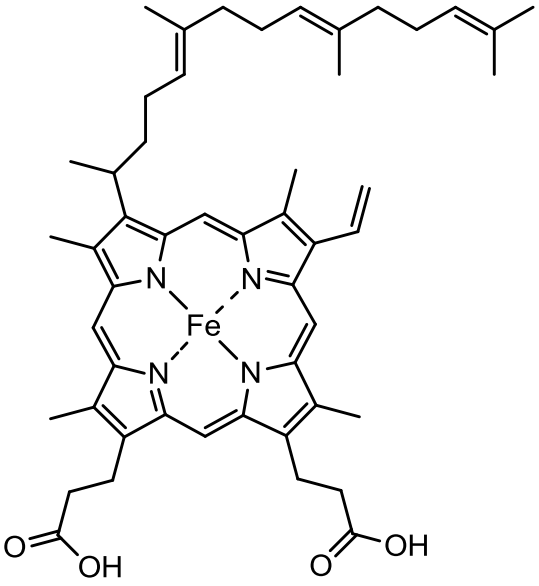

Heme O

Figure 1.3 – Structure of the four most common heme molecules.

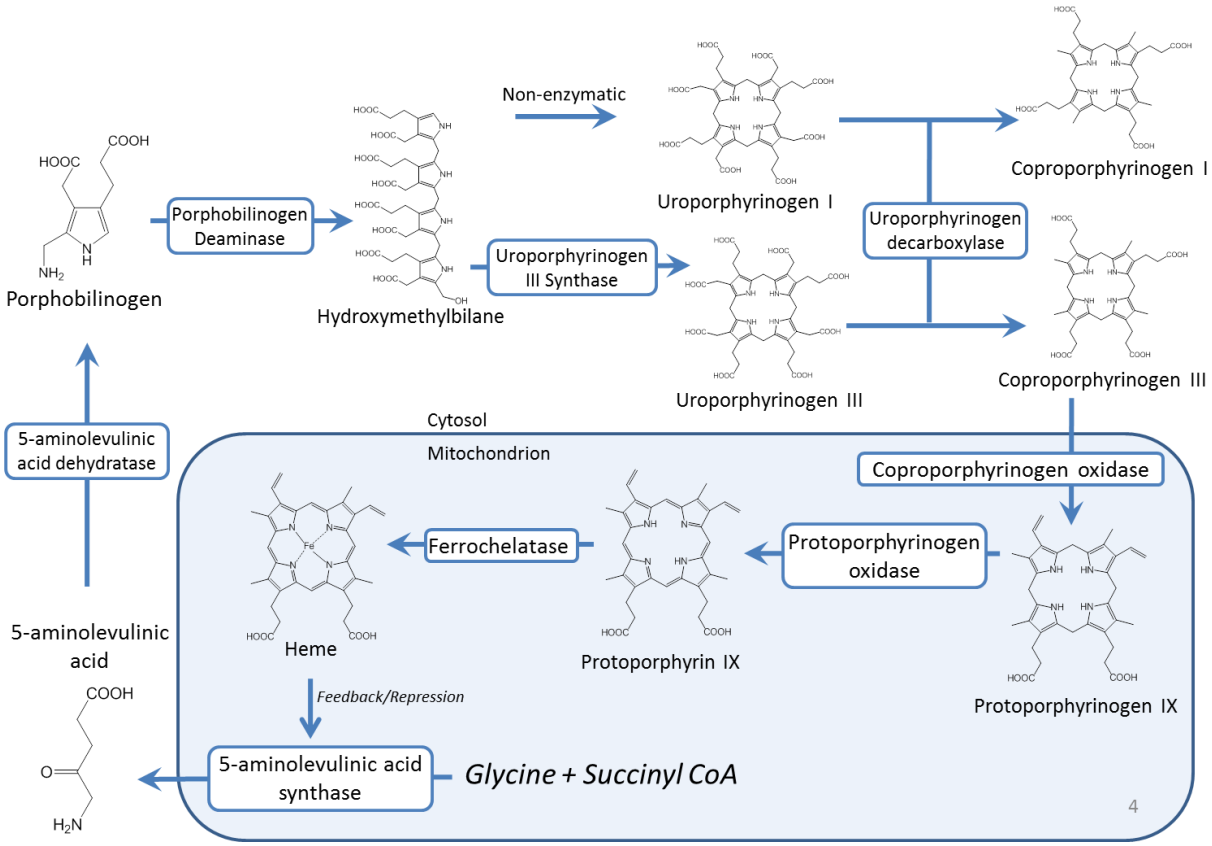

Figure 1.4 – The Heme Biosynthetic Pathway. Enzyme names are enclosed in boxes.

Disease	Enzyme Deficiency	Classification	Inheritance	Symptoms
5-Aminolevulinic acid dehydratase-deficient porphyria (ADP)	5-Aminolevulinic acid dehydratase (ALAD)	Hepatic	Autosomal recessive	Neurovisceral
Acute Intermittent Porphyria	Porphobilinogen Deaminase (PBGD)	Hepatic	Autosomal dominant	Neurovisceral
Congenital Erythropoietic Porphyria	Uroporphyrinogen III Synthase (UROS)	Erythropoietic	Autosomal recessive	Cutaneous photosensitivity
Porphyria Cutanea Tarda	Uroporphyrinogen Decarboxylase (UROD)	Hepatic	Autosomal dominant	Cutaneous photosensitivity
Hepatoerythropoietic Porphyria			Autosomal recessive	
Hereditary Coproporphyria	Coproporphyrinogen III Oxidase (CPO)	Hepatic	Autosomal dominant	Neurovisceral & occasional cutaneous photosensitivity
Variegate Porphyria	Protoporphyrinogen Oxidase (PPO)	Hepatic	Autosomal dominant	Neurovisceral & cutaneous photosensitivity
Erythropoietic Protoporphyria	Ferrochelatase	Erythropoietic	Autosomal dominant	Cutaneous photosensitivity

Table 1.1. Summary of the main characteristics of each type of enzyme deficiency and associated porphyria. Adapted from Anderson *et al.* (12)

REFERENCES

(1) Thompson, J.J. *Philosophical Magazine A* **1912**, *24*, 209.

(2) Cameron, A.E.; Eggers, D.F. *Rev. Sci. Instrum.* **1948**, *19*, 605.

(3) Paul, W.; Steinwedel, H.Z. *Naturforsch A*, **1953**, *8*, 448.

(4) Comisarow, M.B.; Marshall, A.G. *Chem. Phys. Lett.* **1974**, *25*, 282.

(5) Hu, Q.; Noll, R.J.; Li, H.; Makarov, A.; Hardman, M.; Cooks, R.G. *J. Mass Spectrom.* **2005**, *40 (4)*, 430-443.

(6) Paul, W. U.S. Patent 2,939,952, **1960**.

(7) Miller, P.E.; Denton, M.B. *J. Chem. Ed.* **1986**, *63*, 617-622.

(8) Sleno, L.; Volmer, D.A. *J. Mass Spectrom.* **2004**, *39*, 1091-1112.

(9) Fenn. J.B.; Mann, M.; Meng, C.K.; Wong, S.F.; Whitehouse, C.M. *Science*, **1989**, *246*, 64-71.

(10) Wang, N.; Zhao, X.; Lu, Y.; *J. Am. Chem. Soc.* **2005**, *127 (47)*, 16541-16547.

(11) Hederstedt, L.; Lewin, A.; Throne-Holst, M. *J. Bacteriol.* **2005**, *187*, 8361-8369.

(12) Anderson, K.E.; Sassa, S.; Bishop, D.F.; Desnick, R.J. Disorders of Heme Biosynthesis: X-Linked Sideroblastic Anemia and the Porphyrias. In The Metabolic and Molecular Basis of Inherited Disease, 8th ed.; Scriver, C.R., Beaudet, A.L., Sly, W.S., Valle, D., Eds.; McGraw-Hill: New York, 2000; Chapter 124.

(13) Furuyama, K.; HArigae, H.; Kinoshita, C.; Shimada, T.; Miyaoka, K.; Kanda, C.; Maruyama, Y.; Shibahara, S.; Sassa, S. *Blood* **2003**, *101*, 4623-4624.

(14) Gunther, H. *Deutsch. Archiv. Klin. Med.* **1911**, *105*, 89.

(15) Gross, U.; Hoffman, G.F.; Doss, M.O. *J. Inherit. Metab. Dis.* **2000**, *23 (7)*, 641-661.

(16) Elder, G.; Harper, P.; Badminton, M.; Sandber, S.; Deybach, J.-C. *J. Inherit. Metab. Dis.* [Online early access]. DOI: 10.1007/s10545-012-9544-4. Published Online: 11/1/2012.

(17) Gerber, S.A.; Scott, C.R.; Tureček, F.; Gelb, M.H. *J. Am. Chem. Soc.* **1999**, *121*, 1102-1103.

(18) Gerber, S.A.; Scott, C.R.; Tureček, F.; Gelb, M.H. *Anal. Chem.* **2001**, *73*, 1651-1657.

(19) Gerber, S.A.; Scott, C.R.; Tureček, F.; Gelb, M.H. *Bioconjugate Chem.* **2001**, *12*, 603-615.

(20) Zhou, X.F.; Tureček, F.; Scott, C.R.; Gelb, M.H. *Clin. Chem.* **2001,** *47*, 874-881.

(21) Li, Y.; Brockmann, K.; Tureček, F.; Scott, C.R.; Gelb, M.H. *Clin. Chem.* **2004**, *50*, 638-640.

(22) Wang, D.; Eadala, L.; Sadilek, M.; Chamoles, N.A.; Tureček, F.; Scott, C.R.; Gelb, M.H. *Clin. Chem.* **2005**, *51*, 898-900.

(23) Wang, D.; Wood, T.; Sadilek, M.; Tureček, F.; Scott, C.R.; Gelb, M.H. *Clin. Chem.* **2007**, *53*, 137-140.

(24) Blanchard, S.; Sadilek, M.; Scott, C.R.; Tureček, F.; Gelb, M.H. *Clin. Chem.* **2008**, *54*, 2067-2070.

(25) Wolfe, B.J.; Blanchard, S.; Sadilek, M.; Scott, C.R.; Tureček, F.; Gelb, M.H. *Anal. Chem.* **2011**, *83*, 1152-1156.

(26) Duffey, T.A.; Khaliq, T.; Scott, C.R.; Tureček, F.; Gelb, M.H. *Bioorg. Med. Chem. Lett.* **2010**, *20*, 5994-5996.

(27) Khaliq, T.; Sadilek, M.; Scott, C.R.; Tureček, F.; Gelb, M.H. *Clin. Chem.* **2011**, *57*, 128-131.

(28) Duffey, T.A.; Bellamy, G.; Elliott, S.; Fox, A.C.; Glass, M.; Tureček, F.; Gelb, M.H.; Scott, C.R. *Clin. Chem.* **2010,** *56*, 1854-1861.

(29) Wolfe, B.J.; Ghomashchi, F.; Kim, T.; Adam, C.A.; Sadilek, M.; Jack, R.; Thompson, J.N.; Scott, C.R.; Gelb, M.H.; Tureček, F. *Bioconjugate Chem.* **2012**, *23*, 557-564.

(30) Caggana, M; Saavedra, C.; Wenger, D.; Helton, L.; Orsini, J. *Mol. Genet. Metab.* **2008**, *93*, S17.

(31) Orsini, J.; Morrissey, M.A.; Slavin, L.N.; Wojcik, M.l Biski, C.; Martin, M.; Keutzer, J.; Zhang, X.K.; Chuang, W.L.; Elbin, C.; Caggana, M. *Clin. Biochem.* **2009**, *42*, 877-884.

(32) Duffner, P.K.; Caggana, M.; Orsini, J.; Wenger, D.A.; Patterson, M.C.; Crosley, C.J.; Kurtzberg, J.; Arnold, G.L.; Escolar, M.L.; Adams, D.J.; Andriola, M.R.; Aron, A.M.; Ciafaloni, E.; Djukic, A.; Erbe, R.W.; Galvin-Parton, P.; Helton, L.E.; Kolodny, E.H.; Kosofsky, B.E.; Kronn, D.F.; Kwon, J.M.; Levy, P.A.; Miller-Horn, J.; Naidich, T.P.; Pellegrino, J.E.; Provenzale, J.M.; Rothman, S.J.; Wasserstein, M.P. *Pediatr. Neurol.* **2009**, *40*, 245-254.

(33) Wang, Y.; Gatti, P.; Sadilek, M.; Scott, C.R.; Tureček, F.; Gelb, M.H. *Anal. Chem.* **2008**, *80*, 2599-2605.

(34) Wang, Y.; Scott, C.R.; Tureček, F.; Gelb, M.H. *Anal. Chem.* **2008**, *80*, 2606-2611.

Chapter 2

The Direct Assay of δ-Aminolevulinic Acid Dehydratase in Heme Biosynthesis for the Detection of Porphyrias by Tandem Mass Spectrometry.

*Reproduced in part with permission from Anal. Chem., **2010**, 82 (15), 6730-6736.*

Abstract

We report a new assay of human δ-aminolevulinic acid dehydratase (ALAD), an enzyme converting δ-aminolevulinic acid (ALA) into porphobilinogen. The assay is developed for use in the clinical diagnosis of δ-aminolevulinic acid dehydratase-deficient porphyria, a rare enzymatic deficiency of the heme biosynthetic pathway. The assay involves the incubation of erythrocyte lysate with the natural substrate, ALA, followed by quantitative *in situ* conversion of porphobilinogen to its butyramide, and liquid-liquid extraction into a mass spectrometer-friendly solvent. Quantitation of the butyrated porphobilinogen is done by electrospray ionization tandem mass spectrometry, using a deuterium-labeled internal standard. The assay stays well within the range wherein ALAD activity is linear with time. The K_m of ALAD for ALA was measured as 340 μM, and the V_{max} was 19 μM/hr. Average enzyme activity among a random sample of 36 unaffected people was 277 μmol/L erythrocyte lysate/hour with a standard

deviation of 90 µmol/L erythrocyte lysate/hour. The tandem mass spectrometric assay should easily detect the enzyme deficiency, which causes a reduction of activity by 95-99%. The assay shows good reproducibility, low background, requires a simple workup, and uses a commercially available substrate.

2.1 – INTRODUCTION

Heme-based proteins, such as the cytochrome enzymes and hemoglobin, play a vital role in human life. The central molecule of these proteins, heme, is made by the human body in an eight-step, enzyme-assisted pathway. Genetic deficiency in any one of the last seven of these enzymes defines any one of seven rare genetic disorders known collectively as the porphyrias (1). Deficiency in the second enzyme, δ-aminolevulinic acid dehydratase (ALAD), is the cause of ALAD-deficient porphyria (ADP), sometimes referred to as Doss porphyria (2). ALAD catalyzes the formation of porphobilinogen (PBG), a pyrrole intermediate, from two molecules of δ-aminolevulinic acid (ALA) (Figure 2.1). ALAD is the first enzyme in the pathway to be found in the cytosol of the cell, rather than the mitochondrion.

ADP is passed on in an autosomal recessive pattern. Homozygous patients experience a drop in enzyme activity of 95-99%. A heterozygous deficiency results in an enzyme activity level roughly 50% of non-affected people but does not cause ADP. However, the heterozygotes, thought to be as prevalent as 1-2% of certain populations (1), are potentially at risk for greater negative effects of lead poisoning. Lead poisoning results in a lack of ALAD activity as lead reversibly replaces zinc at the enzyme's active sites (3). Clinically, ADP typically presents with acute abdominal pain and peripheral neuropathy, similar to other acute porphyrias (4).

Given its similarities to other porphyrias, ADP is difficult to diagnose. It is differentiated from acute intermittent porphyria (AIP), deficiency in the subsequent enzyme of the pathway, only by increased urinary excretion of PBG. Current assays for ALAD deficiency are, for the most part, based on a method developed by Mauzerall and Granick in 1956 (5). This technique involves reacting the enzymatic product with *p*-dimethylaminobenzaldehyde, or Erlich's reagent, to create a compound detectable by colorimetry or fluorimetry (6-10). A common alternative is a coupled-enzyme assay (11, 12), wherein porphobilinogen is carried further down the biosynthetic pathway to produce hydroxymethylbilane, which spontaneously cyclizes to uroporphyrinogen I, which is then oxidized and detected as uroporphyrin I by fluorimetry. None of the current methods detect porphobilinogen directly, putting them at a clear disadvantage compared to a method that does. Furthermore, it is exceedingly difficult by these methods to distinguish this specific enzyme deficiency from those upstream or downstream.

Previous work in our laboratory has focused on developing procedures for testing enzyme activity levels in human samples using tandem mass spectrometry as a common analytical platform for both clinical diagnostics and newborn screening (13, 14, 15) The methods involve selecting an appropriate biological source of enzyme, typically either isolated and lysed blood cells for diagnostics or dried blood spots for screening, and incubating this sample with the enzyme's substrate, which is often synthetically designed in-lab. The enzymatic product is then quantified by reaction-monitoring tandem mass spectrometry, using a mass-differentiated internal standard. This method takes advantage of the speed and sensitivity offered by mass spectrometry over spectroscopic methods, as well as the specificity and selectivity offered by the use of a tandem instrument. The unique masses used for each assay's product and standard allow for easy multiplexing, as the products of many different assays can be combined into one

injection without any need for chromatographic separation. In particular, we have developed tandem mass spectrometry assays for the detection of acute intermittent porphyria (14), porphyria cutanea tarda, hepatoerythropoietic porphyria, and hereditary coproporphyria (15), which are caused by deficient enzymes in the later stages of the heme biosynthetic pathway. In an effort to provide clinical laboratories with a complete cassette of porphyria assays based on a single analytical platform, we developed a new procedure for the direct assay of ALAD which is reported here.

2.2 – EXPERIMENTAL

Materials. All water used was purified by a Millipore Milli-Q 18MΩ filtering system. Porphobilinogen was purchased from Frontier Scientific (Provo, UT). Butyryl-d_7 chloride and sodium butyrate-d_7 were supplied by C/D/N Isotopes (Pointe-Claire, Quebec). δ-Aminolevulinic acid, dithiothreitol, and all other chemicals were obtained from Sigma-Aldrich (St. Louis, MO).

Isolation of Erythrocytes. Red blood cells were isolated and lysed according to a procedure previously used in this laboratory (14). All procedures regarding human blood followed Institutional Review Board (IRB) protocols and received an IRB approval. Blood was drawn into a vacuum-sealed tube with heparin. Whole blood (3 mL) was then transferred to a 15-mL polypropylene centrifuge tube, 9 mL of 0.9% w/v saline solution was added, the sample was gently shaken, and the tube was centrifuged at 600 x g for 10 minutes. The non-erythrocyte-containing supernatant was discarded, followed by another addition of 9 mL saline. The tube was inverted a few times to gently re-mix the sample, followed by a second centrifugation at 600

x g for 10 minutes. Again the supernatant was discarded, and the cells were washed and centrifuged a third time. Following this third washing, 2.5 mL of red blood cells were drawn from the bottom of the tube and placed in a new 15 mL centrifuge tube. The tube was frozen in a dry ice/acetone bath for 10 minutes and then brought back to room temperature in a water bath. This was repeated two additional times in order to ensure complete cell lysis. The resulting lysate was centrifuged at 13,200 x g for 10 minutes, prior to being split into 50 µL aliquots and stored in 600 µL polypropylene microfuge tubes at -80°C. Before use in assays, the sample tubes were brought back to room temperature and diluted with 450 µL of 18MΩ deionized water. A 50 µL aliquot of this solution was used for assays corresponding to 5 µL of red blood cell lysate per assay.

Internal Standard Synthesis. d_7-Butyrated porphobilinogen (d_7-But-PBG) was synthesized using d_{14}-butyric anhydride, which was made from butyryl d_7-chloride and sodium butyrate-d_7 (both C/D/N Isotopes, 98% D) as follows. Sodium butyrate-d_7 (1 g, 8.54 mmol) was added under stirring to anhydrous tetrahydrofuran (50mL) under an argon atmosphere. Butyryl d_7-chloride (1 g, 8.80 mmol) was added drop-wise, and the system was allowed to react for 72 hours at room temperature. Sodium chloride was filtered off, the solvent was evaporated *in vacuo*, and the residue was purified by short-path vacuum distillation. GC-MS analysis showed that the synthesized d_{14}-butyric anhydride was >98% pure and its D content was 98%.

The d_7-butyrated porphobilinogen internal standard was synthesized from 25.5 mg (8.4×10^{-5} mol) of porphobilinogen using three molar equivalents of d_{14}-butyric anhydride in 5 mL of 0.25 M sodium phosphate buffer (pH 6.8) for 30 minutes at room temperature. HCl (1 M) was

added to reduce the pH to ~2.0, followed by ammonium sulfate (50% w/w of aqueous phase). The product was extracted with ten 2-mL portions of ethyl acetate. The solvent was removed by evaporation under a stream of N_2 and the resulting solid was reconstituted in water for purification by HPLC. A 10 mL/min gradient of 100:0 to 0:100 H_2O:ACN over 30 minutes using a 100x20mm reverse-phase C_{18} column achieved adequate separation to isolate d_7-But-PBG, which eluted at 10.4 minutes. No acid was necessary in the HPLC solvents to separate the compound of interest from the impurities.

Assay Protocol. An amalgamation of previously reported assays was adapted to be compatible with electrospray ionization and tandem mass spectrometry (5, 11). Three hundred microliters of 0.25 M sodium phosphate buffer (pH 6.80), 50 µL of 20 mM dithiothreitol in buffer, and 50 µL of 10-fold diluted red blood cell lysate were combined in a 2.0-mL polypropylene microfuge tube and pre-incubated at 37°C for 15 minutes. Then 100 µL of 5 mM ALA in buffer was added and the mixture was incubated for 60 minutes. After incubation, 5 µL of n-butyric anhydride was added and allowed to react for 30 minutes. Following this *in situ* derivatization, 5 µL of a 275 µM solution of d_7-But-PBG in buffer was added, as well as 100 µL 1 M HCl to reduce the pH to ~2. Four hundred and fifty microliters of water-saturated *n*-butanol and approximately 300 mg ammonium sulfate were then added, the mixture was vortexed for 30 seconds until the ammonium sulfate dissolved, followed by centrifugation for 3 minutes at 13,200 x g to separate the layers. Two hundred microliters of the *n*-butanol supernatant was removed with a syringe to a new 600-µL polypropylene tube, and stored at -80°C. The solution was mixed with 200 µL methanol containing 2% (v/v) formic acid immediately before analysis.

Mass Spectrometry. Analysis was conducted by flow injection with 10 µL injections using a Waters Quattro Micro triple quadrupole mass spectrometer in positive ion mode. Solvent flow to the spectrometer's ESI ion source came from a Waters 1525u HPLC pump, flowing methanol containing 1% (v/v) formic acid at 100 µL/min The instrument was operated using MassLynx software with the following settings: electrospray ionization capillary voltage, 4.00 kV; cone voltage, 38 V; extractor, 2 V; RF lens voltage, 200 mV; source temperature, 80 °C; desolvation temperature, 300 °C; desolvation gas flow, 500 L/hr; dwell time, 250 µs; collision energy, 20 eV; collision gas was argon at 1.97 mTorr.

2.3 – RESULTS AND DISCUSSION

Assay and Sample Work-Up Conditions. Analysis by electrospray ionization mass spectrometry mandates that the sample be in a compatible solvent free of involatile salts and buffers. Therefore, extraction of the enzymatic product into a suitable solvent was necessary. However, porphobilinogen is ionic or zwitterionic at all relevant pH, so derivatization was necessary to allow extraction. We found that porphobilinogen butyramide was effectively extracted into *n*-butanol. *In situ* conversion of porphobilinogen to a butyramide was quantitative by treating the assay mixture with 5 µL of butyric anhydride for 30 min; an internal standard was prepared separately in a similar fashion using d_{14}-butyric anhydride. NMR spectra of the two derivatized compounds are seen in figure 2.2. Of the extraction solvents used, *n*-butanol was superior to ethyl acetate (figure 2.3). The cross-solubility of water and *n*-butanol (roughly 10% soluble) was overcome by using *n*-butanol that had previously been saturated with water. Further, the addition of approximately 300 mg of ammonium sulfate resulted in 89% of

porphobilinogen butyramide being extracted in two steps, including 80% in the first extraction (figure 2.3). One extraction was therefore deemed to be sufficient for the assay. There was no significant difference in extractability between the enzymatic product and the deuterated internal standard. Using anhydrous *n*-butanol without ammonium sulfate decreased the extraction yield to 52% in the first step (figure 2.3).

Previous fluorometric assays for ALAD have shown that dithiothreitol (DTT) increased enzymatic activity (16), by preventing possible inhibition caused by the level of lead in the analyzed blood. However, DTT may suppress the ESI-MS analyte signal, and as such could negatively affect the assay results. Experimental runs with and without DTT showed that the inclusion of 2 mM DTT resulted in a 16% increase of enzyme activity; thus, DTT was included in the final assay mixture. Zinc was also considered as an assay additive, since zinc is used by the enzyme as an active site cofactor. Due to the insolubility of zinc phosphate, this additive required the use of a carbonate buffer. However, using a carbonate buffer rather than phosphate caused nearly a 90% drop in activity and addition of zinc resulted in a further decrease by up to 35% (figure 2.4). Thus, the assays were run in the phosphate buffer system, without any added zinc.

Since a tandem quadrupole mass spectrometer may not be available for immediate analysis in some clinical laboratories, a study was carried out to determine the viability of transporting blood sample to a laboratory with the necessary instrumentation. The relevant shipping conditions were duration and temperature; as such, freshly-drawn whole blood samples were stored at either room temperature or at 4°C for a set of time intervals ranging up to 8 days. Temperatures below 0°C were not considered, as any such storage conditions would prematurely lyse the desired erythrocytes, making it impossible to isolate them. This experiment was

conducted using two separate sets of blood samples, one for each of the two most common blood preservatives (heparin and EDTA). Results show that while some activity is lost within a week at room temperature (regardless of preservative), storing with heparin at 4°C had no effect on the measured enzyme activity level (figure 2.5). Furthermore, both preservatives allowed the retention of enzyme activity, although heparinized samples gave slightly higher levels. Thus, samples should be preserved in heparin and kept at 4°C for any required shipping, to ensure the most reliable determination of enzyme activity.

Mass Spectrometry. Porphobilinogen was found to be readily protonated, sodiated, or potassiated by electrospray ionization. Protonated porphobilinogen readily eliminated ammonia in the electrospray source and on collisional activation. For example, at 5 eV laboratory collision energy, the $(M+H)^+$ ion completely dissociated (figure 2.6). However, due to the above-described solubility issues, underivatized porphobilinogen was not a suitable analyte for this assay. Electrospray of porphobilinogen butyramide mainly produced $(M + Na)^+$ and $(M + K)^+$ ions which were less prone to dissociation than the $(M + H)^+$ ion (Figure 2.7). The $(M + Na)^+$ ion showed the highest intensity for both the derivatized product and internal standard and was therefore used for MS/MS analysis. The $(M + K)^+$ ions, albeit also abundant, showed intensity variations in different assay runs. Collision-induced dissociation of the $(M + Na)^+$ ions gave fragments at *m/z* 275 and 282 for the butyrated enzymatic product and internal standard, respectively, due to loss of 45 Da (COOH) (figure 2.8). The most abundant fragment ion at *m/z* 188 by loss of 131 Da from the butyrated product was due to a combined elimination of butyramide and CO_2. The transitions monitored by MS/MS were *m/z* 319 → 188 for the enzymatic product and 326 → 188 for the internal standard (figure 2.8). Figure 2.9 shows the

tentative scheme for the elimination involving a proton transfer from the proximate carboxyl group onto the butyramide moiety. The fact that both the deuterated and non-deuterated $(M + Na)^+$ precursor ions fragmented to form the same product ion was beneficial because it increased the duty cycle of the measurements, thereby increasing the assay efficiency.

Blank measurements were carried out with samples that lacked erythrocytes or the δ-aminolevulinic acid substrate. In each of these blank measurements, no detectable signal for the *m*/*z* 319 → 188 transition was found by MS/MS. Blank correction in the ALAD assays was therefore unnecessary.

ALAD Enzyme Kinetics. The assay conditions were optimized by varying the assay time, amount of sample, and concentration of substrate to determine the K_m and V_{max}. The time course of the assay was found to be linear up to 4 h (figure 2.10). A 15 min pre-incubation period was necessary to warm up the blood sample before the addition of the substrate. Based on the time dependence we chose a 60-minute incubation for standard assays which produced 800-1000 pmol of porphobilinogen to be readily quantified by tandem mass spectrometry. Experiments were done to find the optimal amount of red blood cell lysate to use. The assay showed a linear product formation with erythrocyte lysate volume (figure 2.11). The most convenient amount was found to be 50 µL of diluted lysate corresponding to 5 µL of the erythrocyte fraction.

Taking into account K_m values previously reported (17, 18) for this enzyme from slightly different biological sources, which ranged from 160 µM in bovine liver to 600 µM in human fetal erythrocytes, the Michaelis-Menten enzyme kinetics parameters were determined by varying the concentration of substrate in the range of 100 µM to 3 mM, with triplicate assays at

each concentration level, and the enzyme activity at each concentration was fitted to a non-linear least-squares model. The K_m was found to be 340 µM, and the V_{max} was found to be 19 µM/hr. Give these values, the concentration used for the assay was set at 1 mM, roughly three times the K_m, to ensure enzyme saturation and reduce any possibility of inter-sample variance in enzyme velocity (figure 2.12).

Clinical Sample Analysis. Following the determination of the relevant parameters, the assay was applied to 35 clinical blood samples, of unknown but varied ages and storage conditions, along with the original blood sample used to elucidate the assay parameters. An equal volume of red blood cells, and subsequently of red blood cell lysate, was used for all samples. The 36 samples showed ALAD activities ranging from 140 to 500 µmol/L erythrocyte lysate/hour. Complete results are seen in table 2.1. The distribution of activities is shown in figure 2.14. The mean enzyme activity was 277 µmol/L erythrocyte lysate/hour, with a standard deviation of 90 µmol/L erythrocyte lysate/hour. The relative standard deviation between injections of the same assay was 3%, while assay-to-assay (using the same enzyme source sample) RSD was 13%.

2.4 – CONCLUSIONS

Tandem mass spectrometry has been shown to be an effective and efficient means for the quantitation of ALAD in red blood cells. The method requires only a one-step liquid-liquid extraction out of aqueous reaction buffer into *n*-butanol and dilution with acidified methanol. Blood samples need not be processed or assayed immediately if stored with heparin at 4°C, and thus can be shipped to a laboratory capable of tandem mass spectrometric analysis without difficulty. Due to the high specificity of tandem mass spectrometry, resulting from the analytes

differing in mass from other compounds in the heme biosynthetic pathway, the assay extract could easily be combined with extracts from other porphyria assays for multiplexed detections in a single injection into the mass spectrometer, improving efficiency. This method offers advantages over earlier more cumbersome, time-consuming, and less specific methods. In spite of some efforts, we have been unable to locate patients who had been previously diagnosed with Doss porphyria (19). It is hoped that the specific assays developed in this laboratory, together with the increasing availability of tandem mass spectrometers in clinical laboratories, will contribute to improved diagnostics of porphyrias in clinical practice.

Acknowledgments. Support of this work by the NIH-NIDDK (Grant R01 DK067859) is gratefully acknowledged. We thank Dr. Martin Sadilek for technical assistance with mass spectrometric measurements.

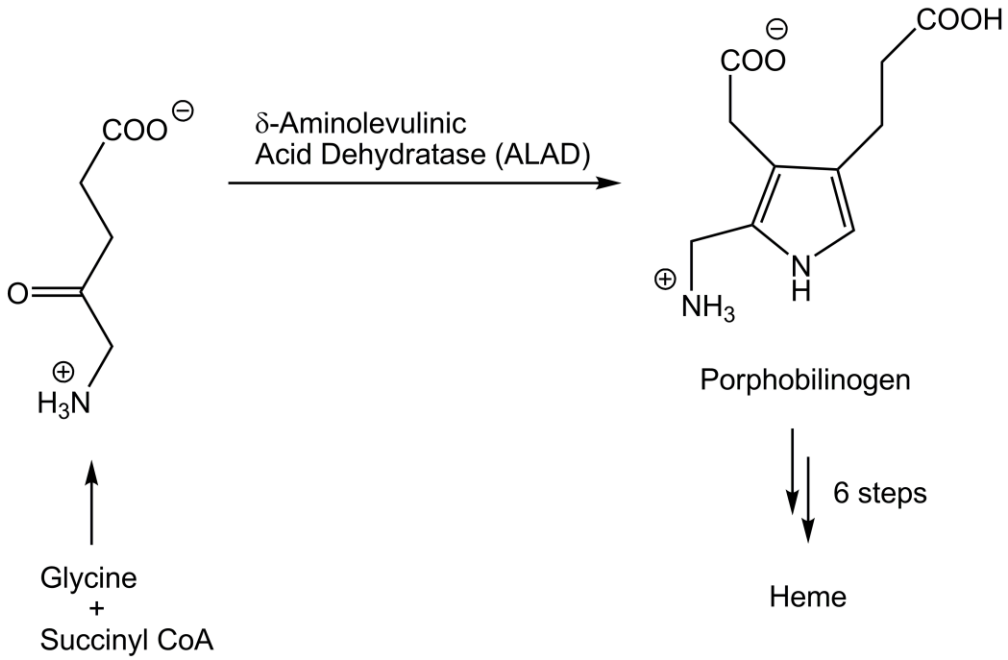

Figure 2.1. The ALAD-catalyzed portion of the pathway.

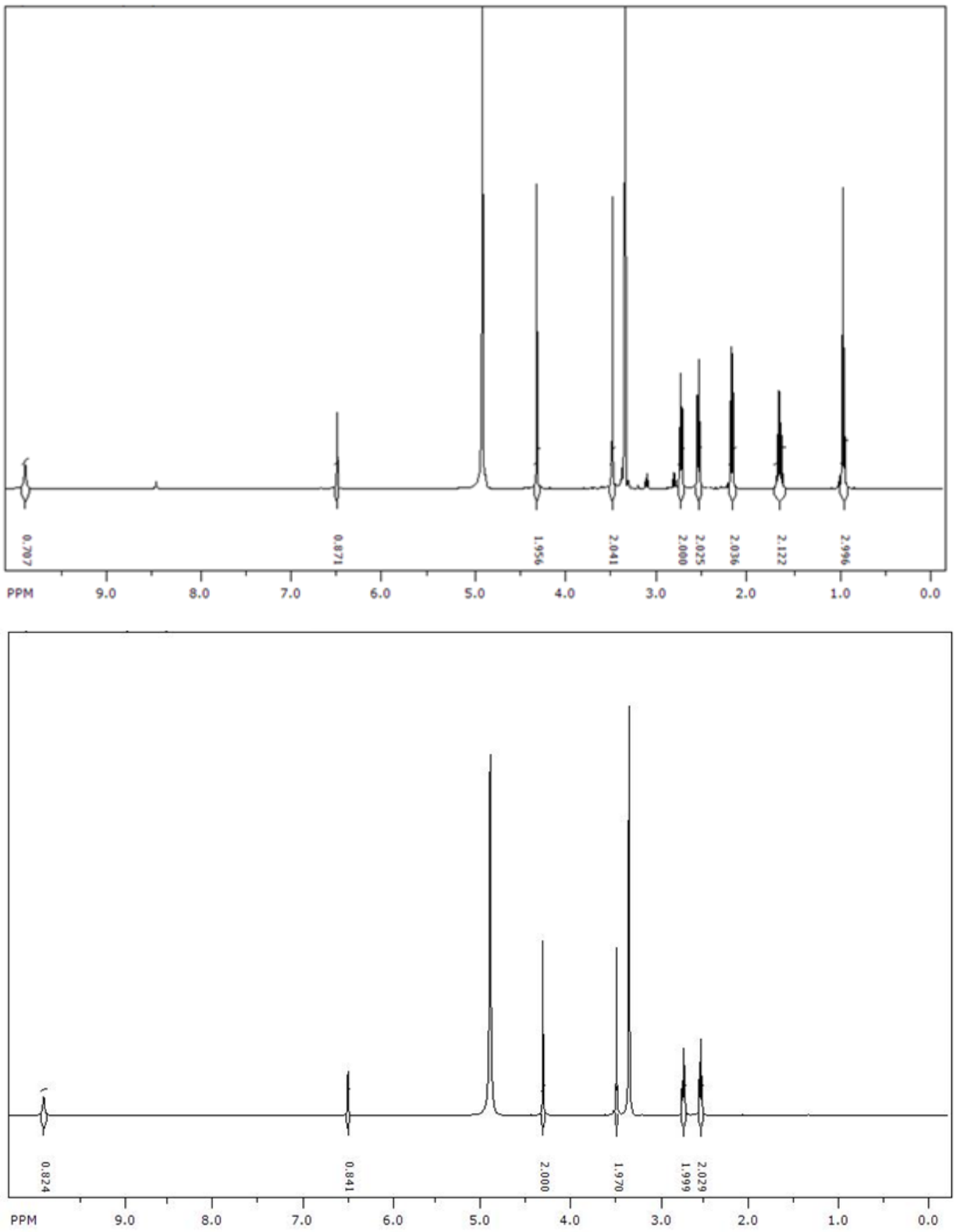

Figure 2.2. 500 MHz NMR spectra of (top) porphobilinogen butyramide and (bottom) d_7-porphobilinogen butyramide. Solvent peaks are seen at 3.4 and 5.0 ppm in both.

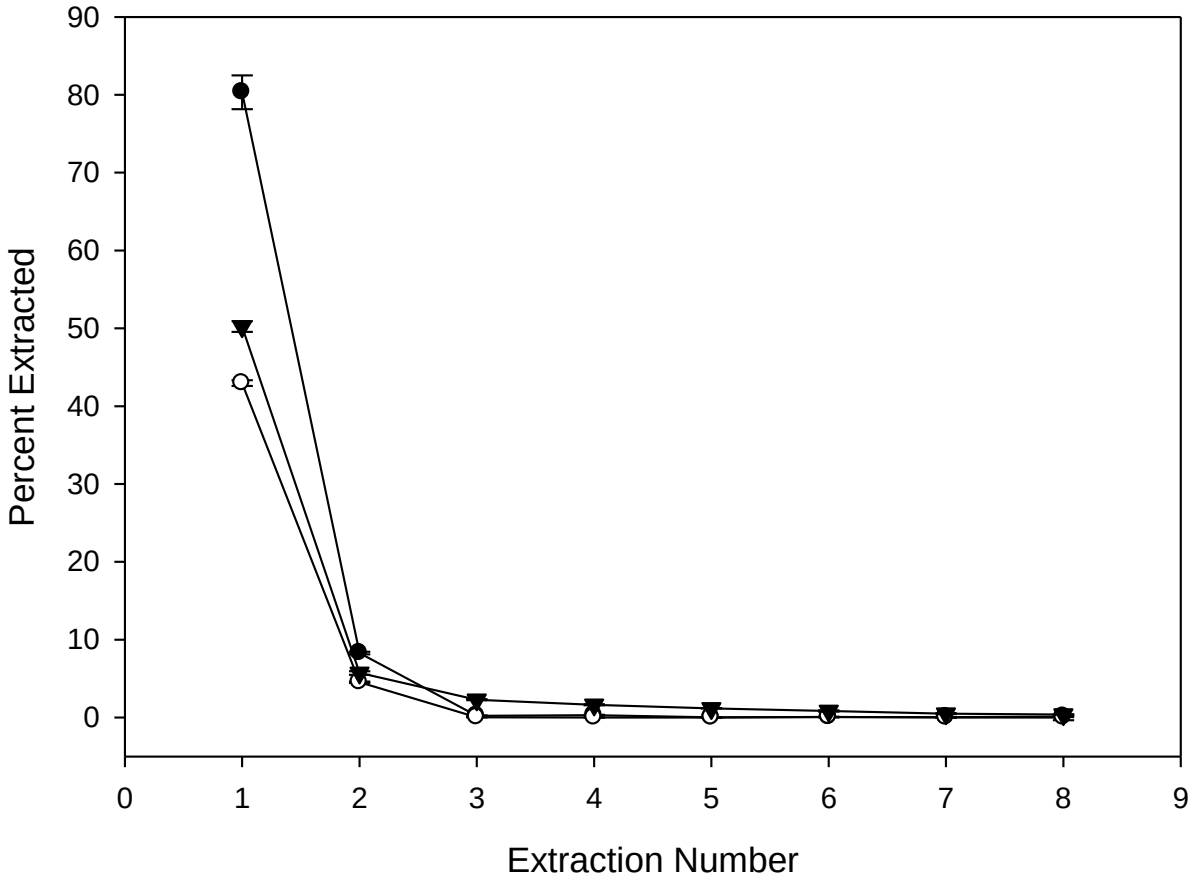

Figure 2.3. Fraction of porphobilinogen butyramide extracted in consecutive extractions by ethyl acetate (open circles), anhydrous *n*-butanol (triangles), and water-saturated *n*-butanol (closed circles). The data error bars are one standard deviation of triplicate measurements.

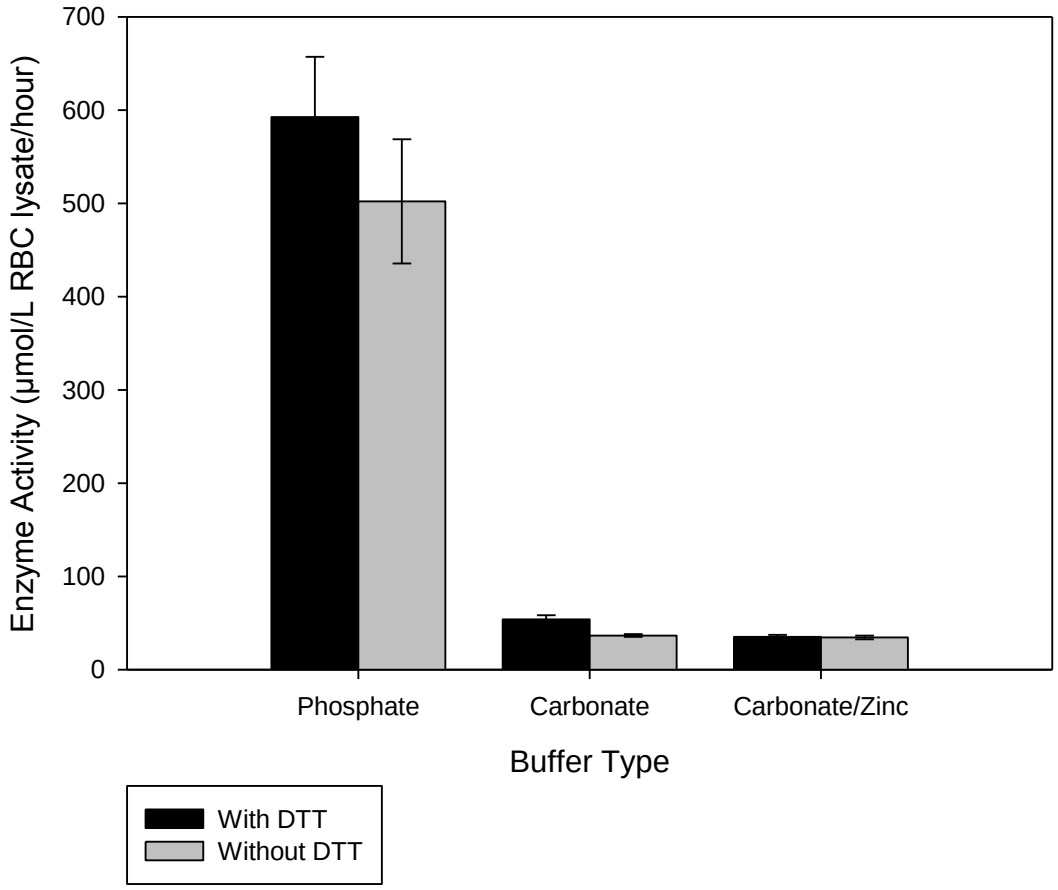

Figure 2.4. Comparison of enzyme activity levels using different buffer systems with or without the inclusion of dithiothreitol. The data error bars are one standard deviation of triplicate measurements.

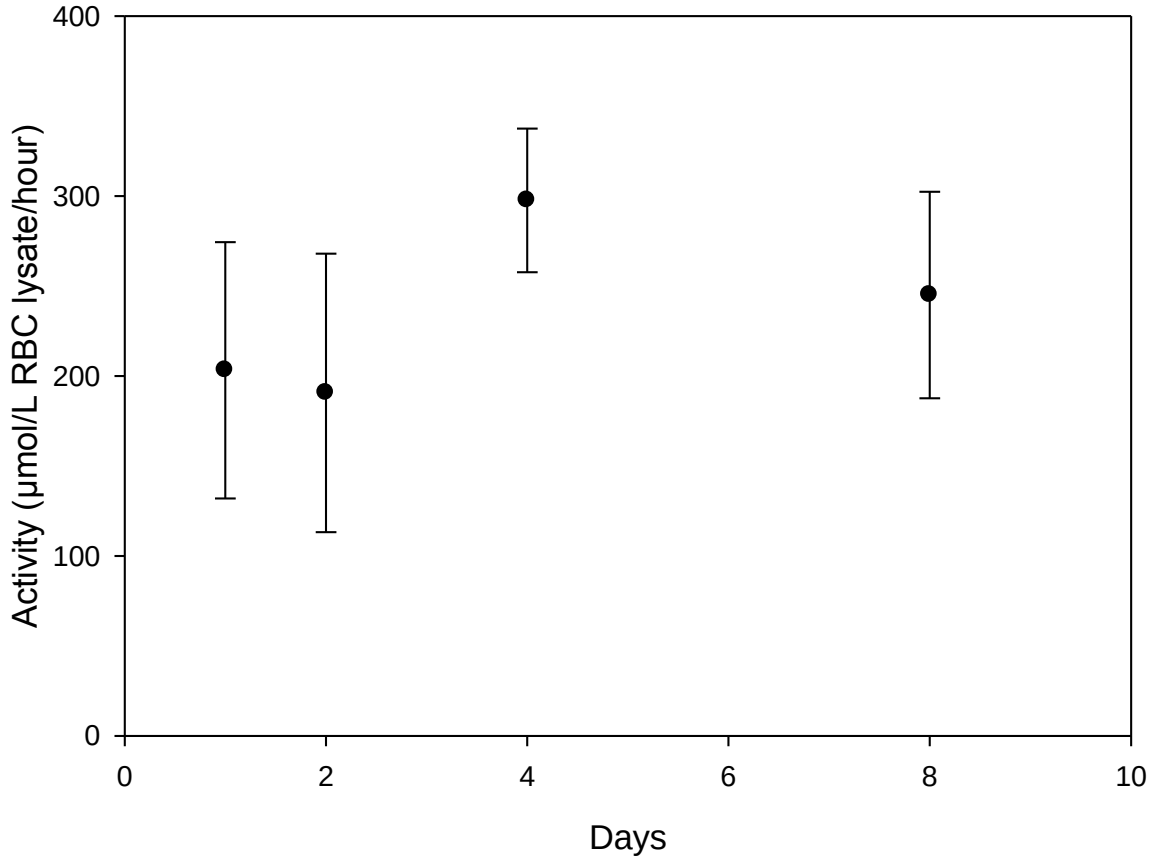

Figure 2.5. Measured activity levels of heparinized blood stored at 4°C for a number of days before erythrocyte isolation and enzyme assay measurement. The data error bars are one standard deviation of triplicate measurements.

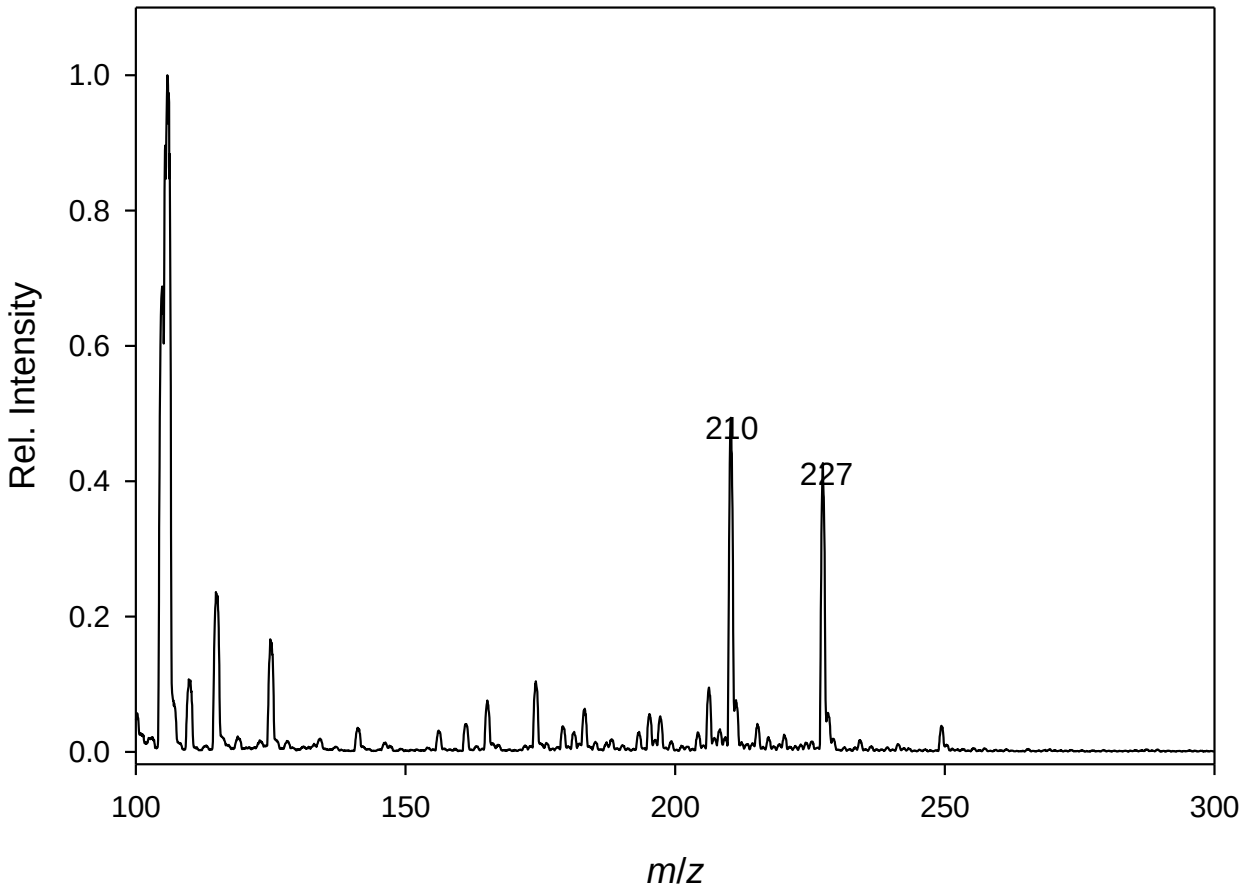

Figure 2.6. Mass Spectrum of underivatized porphobilinogen. [M+H]+ is seen at *m*/*z* 227, and the peak resulting from the loss of ammonia is visible at *m*/*z* 210.

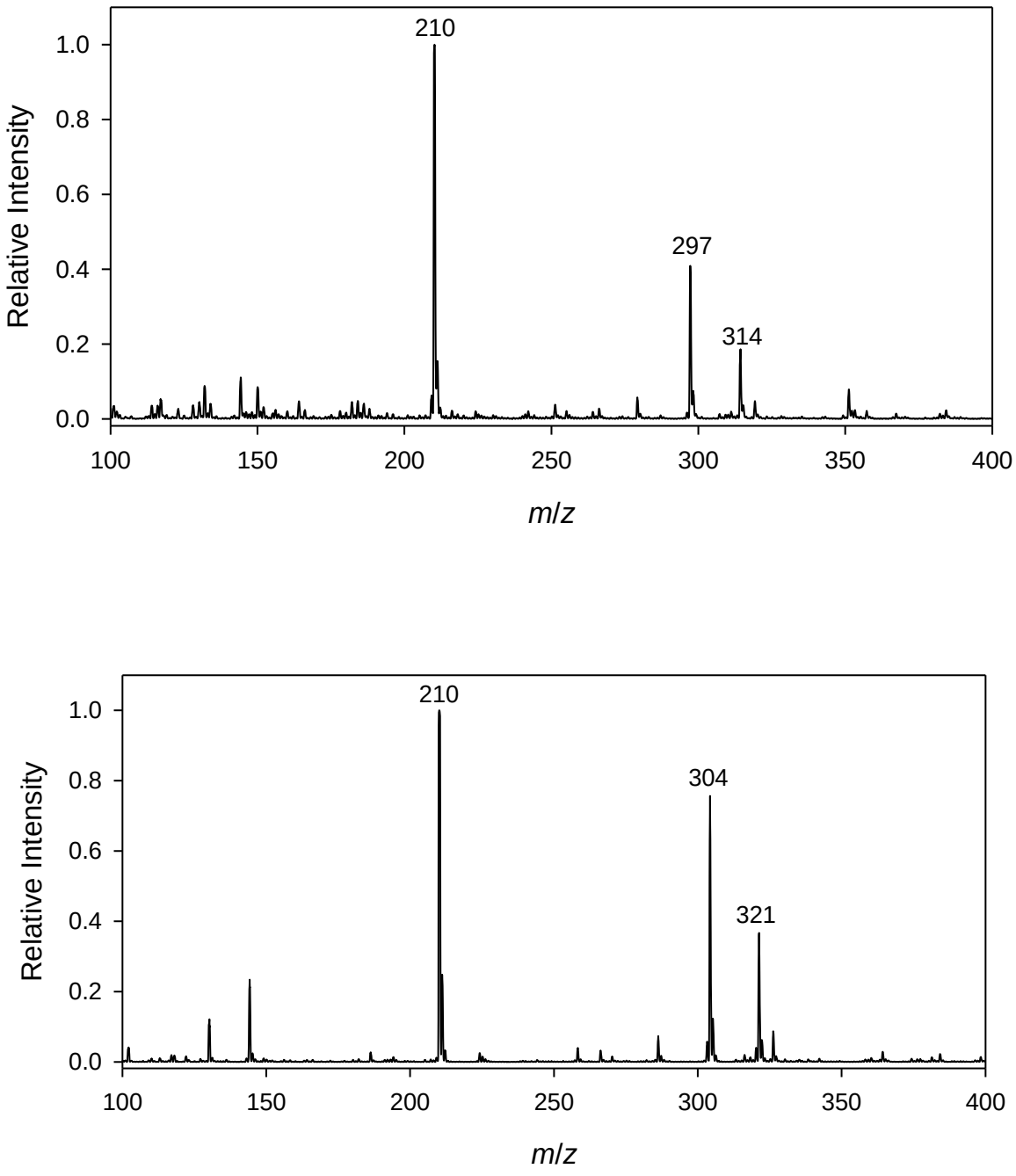

Figure 2.7. ESI-MS of (top) porphobilinogen butyramide and (bottom) porphobilinogen d_7-butyramide.

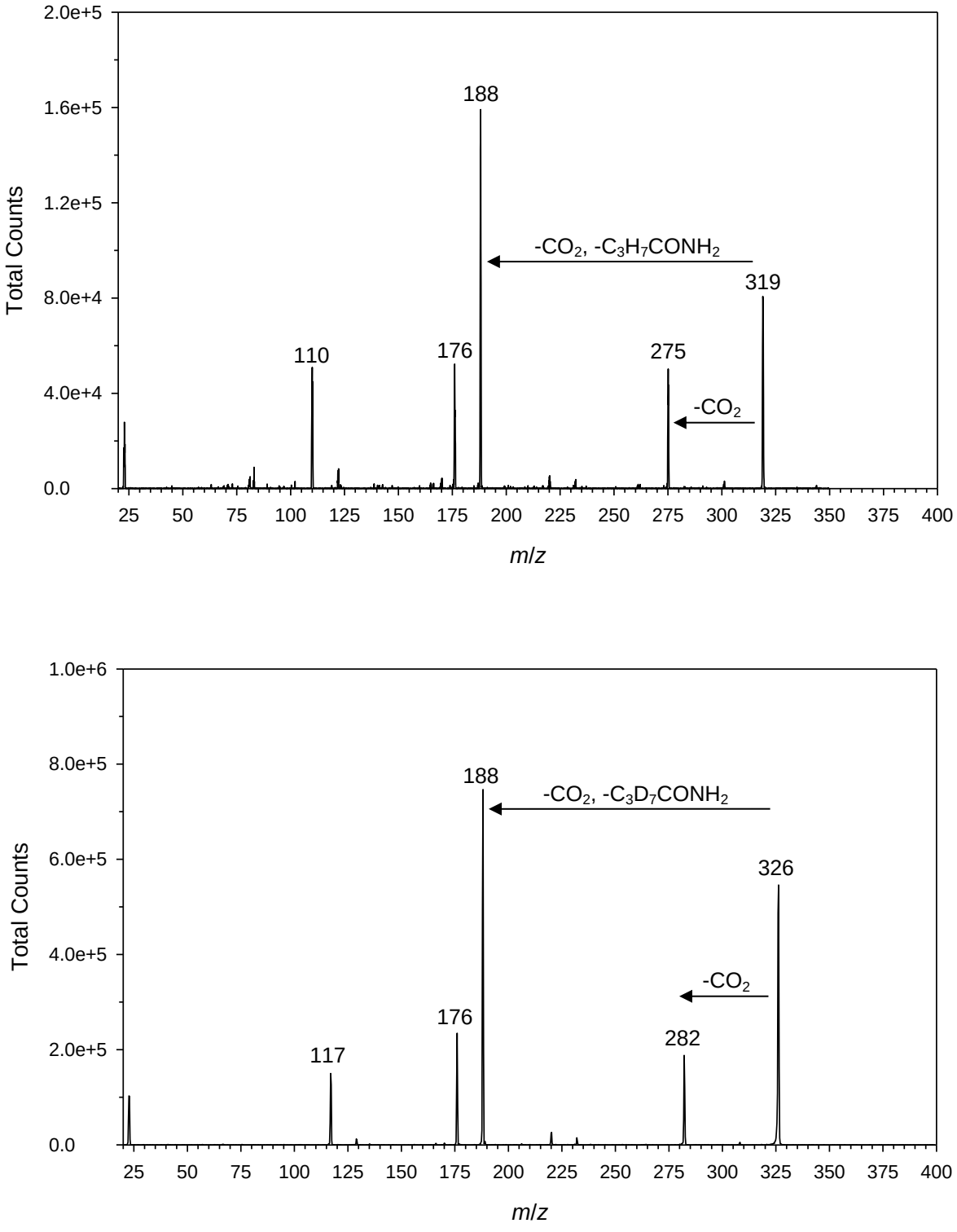

Figure 2.8. Collision induced dissociation mass spectra at 20 eV of $(M + Na)^+$ ions from top: porphobilinogen butyramide (*m/z* 319) and bottom: porphobilinogen d_7-butyramide (*m/z* 326).

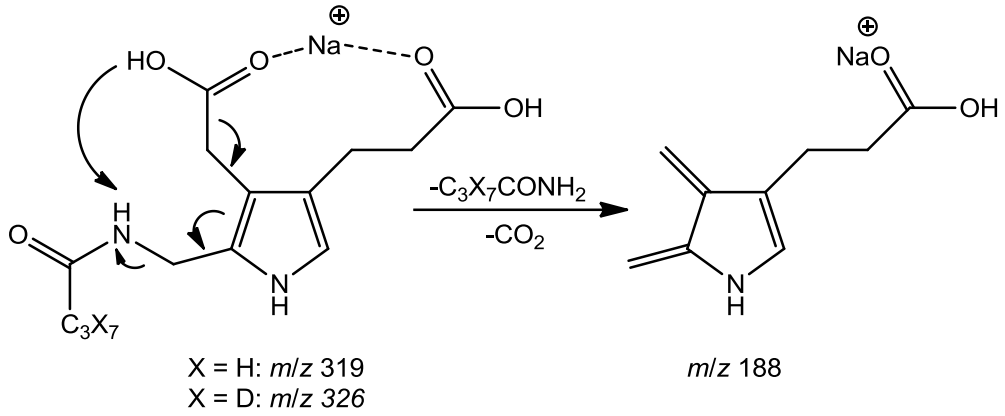

Figure 2.9. Fragmentation mechanism for losses observed in mass spectra.

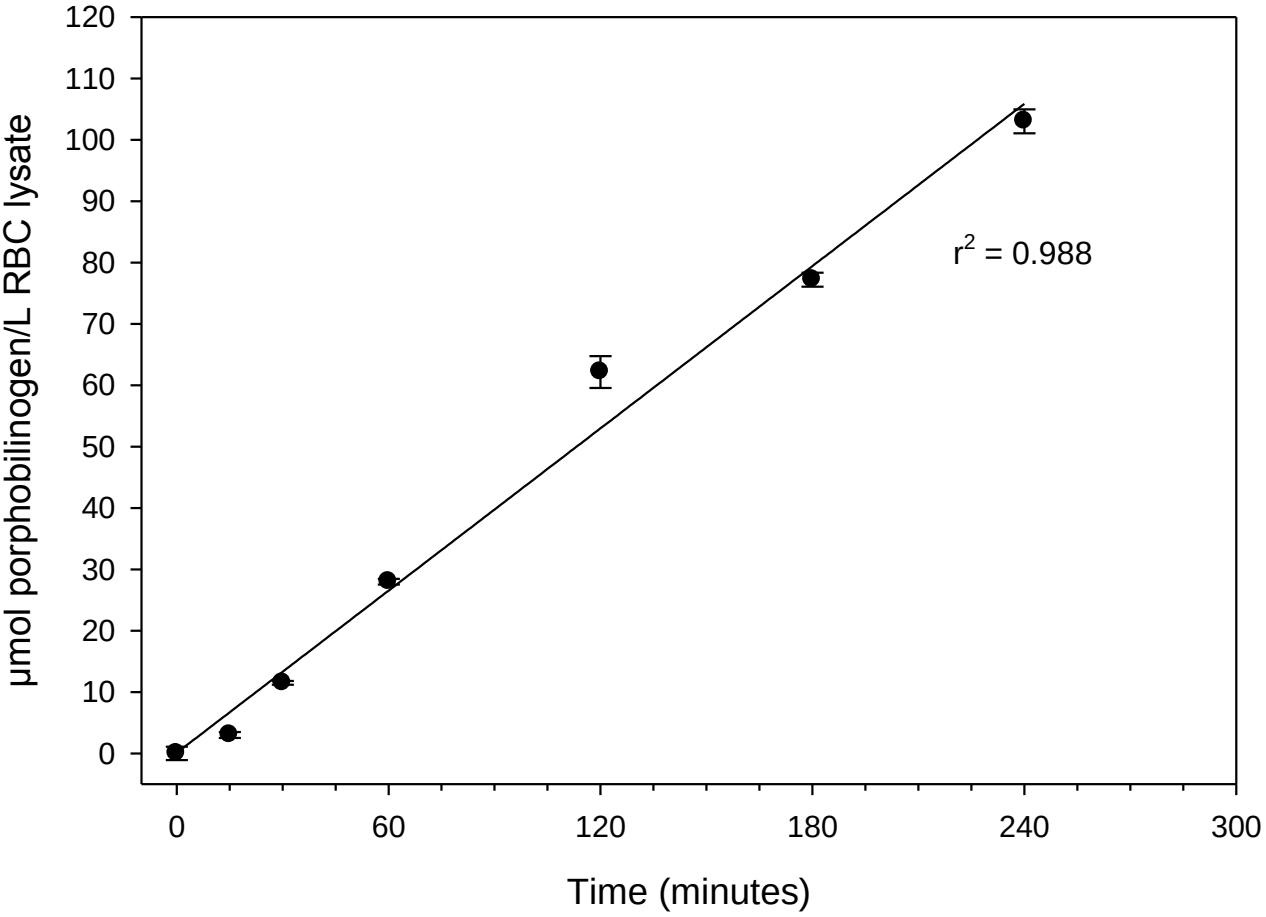

Figure 2.10._ Plot of porphobilinogen product formation against incubation time (after 15-minute preincubation), showing linear dependence, $r^2 = 0.988$. The data error bars are one standard deviation of triplicate measurements.

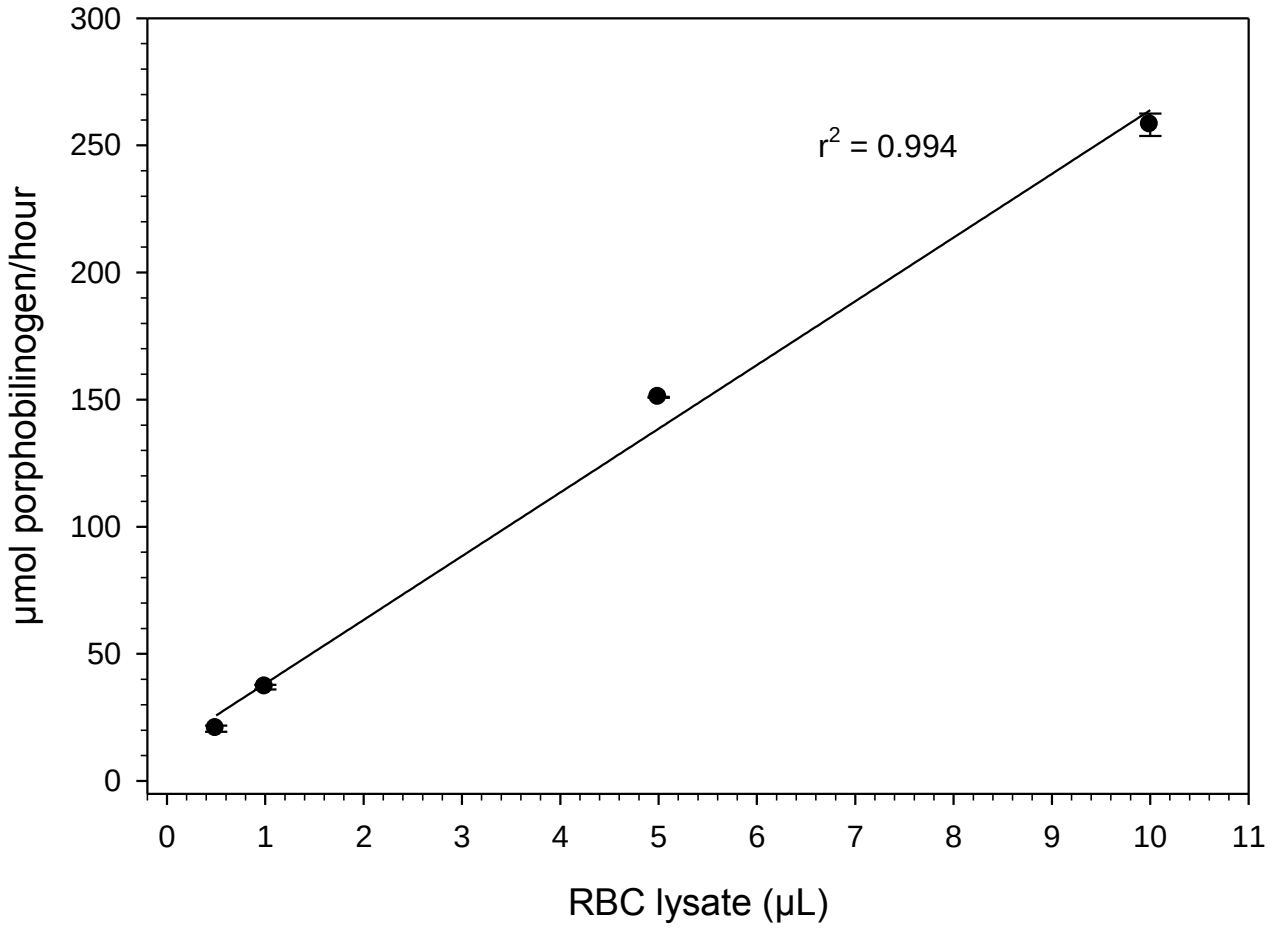

Figure 2.11. Graph of enzyme activity against amount of erythrocyte lysate, showing linear dependence, $r^2 = 0.994$. The data error bars are one standard deviation of triplicate measurements.

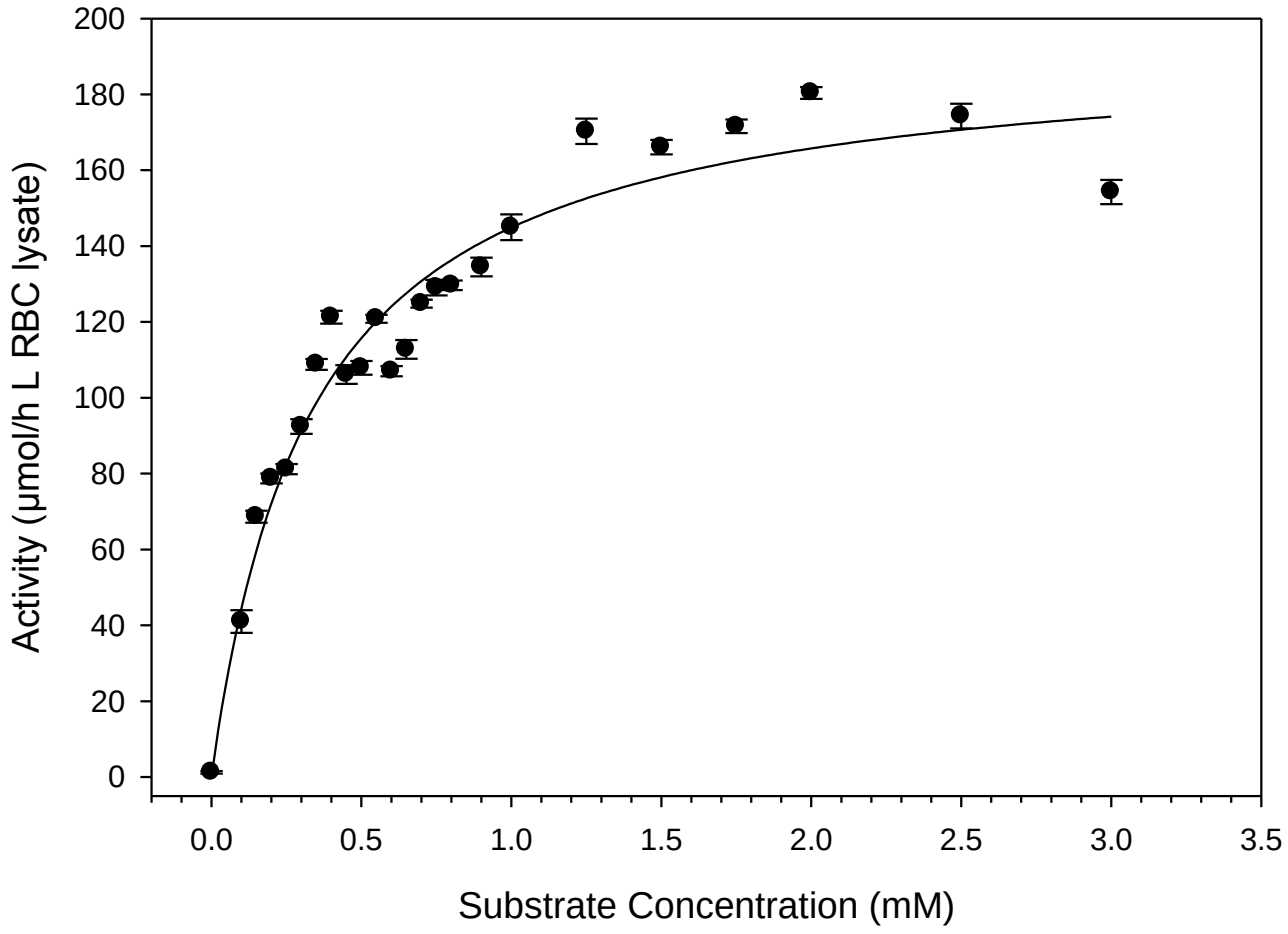

Figure 2.12. Enzyme activity as a function of substrate concentration. The data error bars are one standard deviation of triplicate measurements.

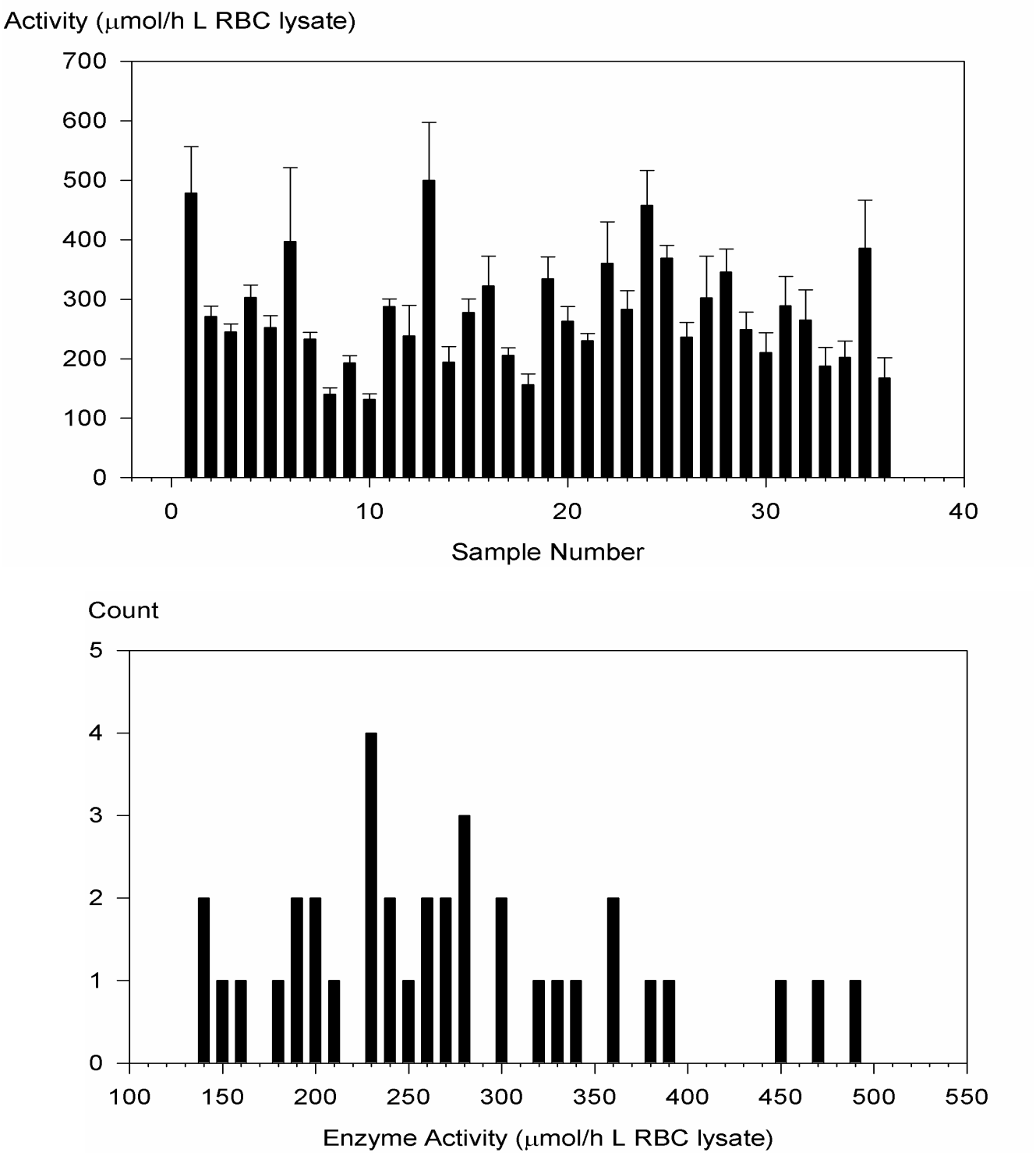

Figure 2.13. Top: Chart of enzyme activity of 36 random erythrocyte samples assayed by tandem mass spectrometry. The data error bars are one standard deviation of triplicate measurements.

Bottom: Distribution of activities among the 36 samples.

Sample ID	Activity (µmol / h * mg lysate)	Standard deviation	Sample ID	Activity (µmol / h * mg lysate)	Standard deviation
1	478	78.3	**19**	334	36.7
2	271	17.3	**20**	263	24.7
3	245	13.2	**21**	230	11.8
4	303	20.5	**22**	360	69.1
5	253	20.0	**23**	283	31.6
6	397	124.3	**24**	458	58.7
7	233	11.3	**25**	369	21.0
8	140	11.2	**26**	236	24.2
9	193	12.3	**27**	302	70.3
10	132	9.3	**28**	346	38.5
11	288	12.5	**29**	249	29.5
12	238	51.1	**30**	210	33.3
13	500	97.2	**31**	289	49.5
14	194	25.9	**32**	265	50.9
15	278	22.7	**33**	188	31.3
16	322	49.9	**34**	202	27.3
17	206	12.2	**35**	385	81.2
18	156	18.0	**36**	168	34.3

Table 2.1. Individual results from 36 anonymous clinical samples. Standard deviations come from triplicate measurements of triplicate assays.

2.5 – REFERENCES

(1) Anderson, K.E.; Sassa, S.; Bishop, D.F.; Desnick, R.J. Disorders of Heme Biosynthesis: X-Linked Sideroblastic Anemia and the Porphyrias. In The Metabolic and Molecular Basis of Inherited Disease, 8th ed.; Scriver, C.R., Beaudet, A.L., Sly, W.S., Valle, D., Eds.; McGraw-Hill: New York, 2000; Chapter 124, pp 2993-2999, pp 3005-3008.

(2) Doss, M.; von Tiepermann, R.; Schneider, J.; Schmid, H. *Klin. Wochenschr*. **1979**, *57*, 1123-1127.

(3) Bird, T.D.; Hamernyik, P.; Nutter, J.Y.; Labbe, R.F. *Am. J. Hum. Genet*. **1979**, *31*, 662-668.

(4) Doss, M.; Sassa, S. The Porphyrias. In Laboratory Medicine. The Selection and Interpretation of Clinical Laboratory Studies; Noe, D.A., Rock, R.C., Eds.; Williams and Wilkins: Baltimore, MD, 1994; Chapter 26, pp 535-553.

(5) Mauzerall, D.; Granick, S. *J. Biol. Chem*. **1955**, *219*, 435-446.

(6) Lüönd, R.M.; Walker, J.; Neier, R.W. *J. Org. Chem*. **1992**, *57*, 5005-5013.

(7) Sassa, S.; Fujita, H.; Kappas, A. *Pediatrics*, **1990**, *86*, 84-86.

(8) Anderson, P.M.; Desnick, R.J. *J. Biol. Chem*. **1979**, *254*, 6924-6930.

(9) Wigfield, D.C.; Farant, J.-P. *Clin. Chem*. **1981**, *27*, 100-103.

(10) Wigfield, D.C.; Farant, J.-P.; Goldberg, C.; MacKeen, J.E. *J. Anal. Tox*. **1981**, *5*, 57-61.

(11) Giampetro, P.F.; Desnick, R.J. *Anal. Biochem*. **1983**, *131*, 83-92.

(12) Bishop, D.F.; Desnick, R.J. *Method Enzymol*. **1986**, *123*, 339-345.

(13) Gelb, M. H.; Tureček, F.; Scott, C. R.; Chamoles, N. A. *J. Inherited Metab. Dis*. *2006*, **29**, 397-404.

(14) Wang, Y.; Gatti, P.; Sadilek, M.; Scott, C. R.; Tureček, F.; Gelb, M. H. *Anal. Chem.* **2008**, *80*, 2599-2605.

(15) Wang, Y.; Scott, C. R.; Gelb, M. H.; Tureček, F. *Anal. Chem*. **2008**, *80*, 2606-2611.

(16) Sassa, S.; Granick, S.; Kappas, A. *Ann. NY Acad. Sci*. **1975**, *244*, 419-439.

(17) Sassa, S. *Enzyme* **1982**, *28*, 133-145.

(18) Chang, C. S.; Sassa, S. *Blood* **1985**, *65*, 939-944.

(19) Akagi, R.; Kato, N.; Inoue, R.; Anderson, K. E.; Jaffe, E. K.; Sassa, S. *Mol. Genet. Metab.* **2006**, 87, 329–336.

Chapter 3.

The Direct Assay of the Enzyme Ferrochelatase for the Detection of Erythropoeitic Protoporphyria by Tandem Mass Spectrometry

ABSTRACT

A new assay is reported for the enzyme ferrochelatase, which catalyzes the insertion of iron (II) into protoporphyrin IX to create heme. The assay is developed for use in the clinical diagnosis of erythropoietic protoporphyria, a rare enzymatic deficiency of the heme biosynthetic pathway. The assay is carried out by incubating lymphocyte lysate with two non-natural substrates, cobalt (II) chloride and mesoporphyrin IX, followed by a liquid-liquid extraction into a solvent appropriate for the mass spectrometer. Quantitation of the cobalt-mesoporphyrin IX complex is accomplished by electrospray ionization tandem mass spectrometry, using a mass-differentiated internal standard. The assay is performed within the time limits of the linear range of activity for this enzyme, requiring 20 hours of incubation to maximize the product. The K_m of cobalt (II) chloride and mesoporphyrin IX were found to be 43.0 µM and 27.4 µM, respectively. The average enzyme activity of a group of 11 unaffected individuals was 2.8 nmol/mg lysate * hr, and the standard deviation was 1.1 nmol/mg lysate * hr. The assay shows good reproducibility, requires only a simple workup, and uses commercially available substrates.

3.1 – INTRODUCTION

Heme-based compounds, such as hemoglobin, vitamin B_{12}, and the cytochrome enzymes, play a vital role in human life. The common functional group to all these, heme, is a tetrapyrrole ring-shaped molecule synthesized in the body through an eight-step, enzyme-assisted pathway. Genetic deficiency in any of the last seven of these enzymes defines the set of conditions known as the porphyrias (1). The final enzyme in the pathway, ferrochelatase, catalyzes the insertion of ferrous iron into protoporphyrin IX to make the finished heme (figure 3.1). Deficiency in this enzyme causes the disease known as erythropoietic protoporphyria (EPP) (2). Ferrochelatase is one of four heme-associated enzymes found in the mitochondrion of the cell.

Erythropoietic protoporphyria is inherited in an autosomal dominant pattern. While this would ordinarily mean that patients with the disease have an enzyme activity level 50% of non-affected people, symptomatic patients are more commonly found to have activity decreased by 75-85%. It is considered the third most common form of porphyria, and is the most common of the erythropoietic types. The primary symptom is photosensitivity, which tends to stay at a stable level for many years, but it can also cause severe liver damage due to the accumulation of protoporphyrin. Photosensitivity caused by this disease is most commonly treated with beta-carotene (3).

Due to the non-specificity of its primary symptom, EPP is difficult to definitively diagnose; in fact, it was not fully described as a separate porphyria until 1961 (4). Further, the accumulation of protoporphyrin occurs in many other diseases, including some other porphyrias. Current diagnostic methods are thus either non-specific or highly cumbersome. Assays exist, but are not used extensively for clinical diagnosis. A protoporphyrin disappearance assay is common, but given the susceptibility of protoporphyrin to degrade under UV radiation is not

specific. A radiometric assay using ^{59}Fe has also been used (5), but requires cumbersome procedures that guarantee complete recovery of the radioactive product. The specific genetic changes that can cause EPP are known, and hence it can be diagnosed through sequencing, but this is both time-consuming and expensive, and would obviously not work for any novel mutations.

Previous work in our laboratory has focused on the development of procedures for determining enzyme activity levels in human samples using tandem mass spectrometry as a common analytical platform for both clinical diagnostics and newborn screening (6,7). The methods involve the selection of an appropriate biological source (typically blood sample lysate for clinical diagnostics and dried blood spots for newborn screening), and incubating this sample with a selected substrate or substrates, frequently designed in-lab specifically for this purpose. The enzymatic product is then quantified by reaction-monitoring mass spectrometry, using a mass-differentiated internal standard. This method takes advantage of the speed and sensitivity offered by mass spectrometry over spectroscopic methods, as well as the specificity and selectivity offered by a tandem instrument. Further, the unique masses used for each assay's product and internal standard allow for easy multiplexed analysis, as the products of many different assays can be injected in the same sample without any need for chromatographic separation.

Our previous work within the family of porphyrias has led to mass spectrometric diagnostic assays for acute intermittent porphyria (8), porphyria cutanea tarda (9), hepatoerythropoietic porphyria (9), hereditary coproporphyria (9), and δ-aminolevulinic acid dehydratase-deficient porphyria (10). Here, that list is expanded with the development of a diagnostic assay for erythropoietic protoporphyria.

3.2 – EXPERIMENTAL

Materials. All water used was purified by a Millipore milli-q 18 MΩ filtering system. Mesoporphyrin IX dihydrochloride, protoporphyrin IX dihydrochloride, and cobalt protoporphyrin IX dihydrochloride were purchased from Frontier Scientific (Provo, UT). Ficoll-Paque PLUS™ separation medium was obtained from GE Healthcare Life Sciences (Pittsburgh, PA). Oxygen gas was procured from Praxair (Seattle, WA). Cobalt (II) chloride, glutathione, n-butanol, and all other chemicals used were obtained from Sigma-Aldrich (St. Louis, MO).

Isolation of Lymphocytes. Using a procedure previously established in our laboratory as a starting point, lymphocytes were separated from whole blood by the following method. Whole blood was drawn into a vacuum tube optionally containing a preservative (EDTA, heparin, or ACD). Separately, three milliliters of Ficoll-Paque PLUS solution was added to a Leucosep 15-mL round-bottom graduated polypropylene tube containing a support disc at approximately the 3-mL level. The whole blood was mixed in a 1:1 ratio with phosphate-buffered saline (PBS). Four milliliters of the diluted blood was gently added by plastic transfer pipet to the 15-mL tube. The tube was then centrifuged at 360 x g for 30 minutes, using a climate-controlled centrifuge holding the chamber's temperature between 18° and 20° C for the entire duration. After centrifugation, the visible band of mononuclear cells between the serum layer and separation medium layer was transferred by pipet to a fresh 15-mL conical centrifuge tube. The sample was diluted to 10 milliliters with PBS, vortexed for 30 seconds, and centrifuged under the same conditions as before for 10 minutes. The supernatant was decanted away from the now-pelletized mononuclear cells. Five milliliters of chilled (~4° C) 18 MΩ-resistance deionized water was added to the tube, and the sample was vortexed for 30 seconds, to lyse any remaining

red blood cells. After vortexing, five milliliters of 1.8% w/v saline was added, and the sample was centrifuged as before. The supernatant was discarded, and the cells were washed one final time with 0.9% w/v saline before a final centrifugation and discarding of the supernatant. The resulting cell pellet was either used immediately or stored at -80° C.

Synthesis of Cobalt (II) Mesoporphyrin. The cobalt (II) complex of mesoporphyrin used in calibration was artificially synthesized using cobalt (II) acetate, according to the method described by Taylor (11). Cobalt (II) acetate was dissolved glacial acetic acid, approx. 1 mg/mL. The mixture was heated to 80°C with stirring. Separately, mesoporphyrin IX dihydrochloride was dissolved in 50°C glacial acetic acid, also at approx. 1 mg/mL. Regardless of absolute amounts, cobalt (II) acetate was in 10x molar excess relative to mesoporphyrin. Under an atmosphere of argon, the dissolved mesoporphyrin was added dropwise to the stirring cobalt (II) acetate at a rate of roughly 10 mL/hr. Following the addition, the reaction flask was cooled in an ice-water bath. Just as the acetic acid began to freeze, the flask was removed from the bath. The now crystallized crude product was collected on a fritted funnel, using vacuum filtration; the crystals were washed with chilled acetic acid. The funnel was dried overnight in a vacuum desiccator over KOH and NaOH pellets. The desired product was isolated by silica gel chromatography, using an 8:5:1 mixture of methanol, chloroform, and water as the isocratic eluting solvent.

Protein Concentration Measurement. The total protein concentrations of the lymphocyte samples were measured by the Bradford dye assay. Ten microliters of sample were added to a 1.5 mL microfuge tube, followed by 500 μL of a 4:1 mix of water and concentrated Bradford

reagent. The tube was vortexed briefly, and allowed to react for 45 minutes. Five hundred microliters of the reacted mixture was then combined with 500 µL water, and the absorbance at 595 nm was taken. Readings were compared to a calibration curve developed from five samples ranging between 0 and 1 mg/ml BSA, assayed in the same way.

Assay Protocol. A combination of previously reported assays was adapted for compatibility with analysis by electrospray ionization mass spectrometry. Two hundred microliters 0.9% w/v saline was added to a lymphocyte pellet, created as described above; cells were resuspended by brief, low-speed vortexing. The cells were then lysed by 20 ultrasonic pulses. Fifty microliters of the lysate were combined in a 1.5 mL polypropylene microfuge tube with 275 µL 0.1 M Tris-HCl buffer (pH = 8.10) containing 0.5% v/v Tween 80, 100 µL of 475 µM mesoporphrin IX dihydrochloride in buffer, and 50 µL of 475 µM cobalt (II) chloride in buffer. This reaction mixture was incubated at 37° C for 20 hours. Following incubation, the reaction was stopped by the addition of 25 µL of 1.000 M HCl. Twenty-five microliters of 200 µM cobalt (III) protopophyrin was then added, for use as an internal standard. To oxidize the cobalt (II) mesoporphyrin complex to cobalt (III), which contains a permanent ion and as such is much more detectable by mass spectrometry, the mixture was then bubbled with oxygen gas for 20 minutes. Liquid-liquid extraction was then performed to remove the compounds of interest to a more instrument-compatible matrix. Seven hundred microliters of water-saturated *n*-butanol was added to the microfuge tube. The tube was then vortexed at high speed for thirty seconds, followed by centrifugation for three minutes at 13,200 x g. An aliquot of the supernatant was taken and combined with an equal volume of acetonitrile for analysis by mass spectrometry.

Mass Spectrometry. Analysis was conducted by flow injection (10 µL injection volume) using a Waters Quattro Micro tandem quadrupole mass spectrometer in positive ion mode. Solvent flow is produced by a Waters 1525u HPLC pump, flowing a 50:50 mix of acetonitrile and 18 MΩ deionized water at 200 µL/min. The water was included to decrease clogging. The instrument was operated using MassLynx software with the following settings, which were experimentally optimized: electrospray ionization capillary voltage: 4.00 kV; cone voltage: 60 V; extractor: 6 V; RF lens voltage: 200 mV; source temperature: 80° C; desolvation temperature: 300° C; desolvation gas flow: 300 L/hr; dwell time: 100 µs; collision energy: 50 eV; collision gas: argon, 1.97 mTorr.

3.3 – RESULTS AND DISCUSSION

Assay and Work-up Conditions. Under natural conditions, ferrochelatase catalyzes the insertion of ferrous iron into protoporphyrin IX. However, it is well-known that the enzyme can function both with a range of other 2+ metals *and* with other related porphyrins (12). Porra and Ross have shown, in fact, that the enzyme's activity level increases six- to eight-fold when using mesoporphyrin IX as a substrate instead (13). Mesoporphyrin IX differs from protoporphyrin IX solely in the "side-chains" of the decarboxylated porphyrin rings; mesoporphyrin IX features two ethyl groups, while protoporphyrin IX features two vinyl groups (figure 3.2). Experiments were conducted to verify this activity increase; while almost no activity could be found using protoporphyrin IX there was clear activity with mesoporphyrin IX, and so it was chosen as the substrate for this assay. As for the metal, while the enzyme prefers ferrous iron, its multiple naturally-occurring isotopes had the potential to complicate the mass spectrometry. Cobalt was chosen as a substrate in its place, for two primary reasons: cobalt is monoisotopic, which

clarifies the mass spectrometry, and the cobalt-bound versions of protoporphyrin IX and mesoporphyrin IX do not naturally occur, and hence don't interfere with the assay or cause high background signal. The use of cobalt and mesoporphyrin IX as substrates also allowed for the use of the commercially-available cobalt protoporphyrin IX as a mass-differentiated internal standard.

Electrospray mass spectrometry requires that the sample be in a compatible solvent, free of involatile salts and buffers. As such, extraction from the aqueous assay buffer into a more appropriate solvent was necessary. This was mildly complicated by the presence of the two carboxylic acids on both analyte and internal standard, which give the cobalt (III)-bound compounds zwitterionic character; however, reducing the pH from 8.1 (as required for enzyme activity) to ~2, through the addition of 25 µL 1.000 N HCl eliminated any problems. Previous work had indicated that either ethyl acetate or water-saturated n-butanol were likely to be successful extraction solvents; for these particular compounds, only n-butanol extraction was successful.

Previous assays have indicated that the inclusion of an antioxidant compound is necessary to retain enzyme function. Typically, this has been the tripeptide glutathione; hence, its inclusion in the assay here was investigated. Assays were attempted in triplicate either containing or not containing glutathione at the previously-used concentration of 1 mM, and each sample was then analyzed with three injections. Activity levels between the two types of samples were not significantly different from each other, with the non-glutathione samples having roughly 5% increased activity over the ones containing it; as such, it was not included in the final assay procedure (figure 3.3).

Palmitic acid has, in some cases, been found to increase the level of enzyme activity by as much as an order of magnitude (14, 15). The inclusion of palmitic acid was therefore investigated here as an additive to increase the measured activity levels, with the goal of increasing the signal-above-blank level. The amount included, which produced a concentration of 20 μM, was based on the amounts previously reported to impact enzyme activity. Unfortunately, no change in activity was observed (figure 3.4)

While enzyme functions with metals in the 2+ oxidation state, this leaves the resulting complex as a neutral species. It would therefore simplify the mass spectrometry greatly to oxidize the central metal to a 3+ species, giving the complex a permanent +1 charge. Here, this was accomplished by bubbling oxygen gas through the sample after incubation, acidification, and the addition of the internal standard, but before the addition of the extraction solvent. Experiments were done that bubbled oxygen for 20 minutes and for 60 minutes, which were compared to a non-oxygenated control. The gas flow rate was not measured; rather, as high a flow rate as possible through a 21-gauge needle without causing the sample to bubble over (due to persistent bubbles formed because of the detergent in the buffer) was used. At 20 minutes, there was a 2.5x increase in the measured activity level; after 60 minutes, it was reduced to 1.5x, probably due to oxidative destruction of the compound (Figure 3.5). Twenty minutes was deemed an appropriate length of time for the final assay parameters.

Mass Spectrometry. After oxidation, the cobalt mesoporphyrin complex was primarily seen in the mass spectrometer as the permanent ion without the addition of any protons, sodium ions, etc., at *m*/*z* 623. The peak at *m*/*z* 624, roughly 40% of the base peak, matches well with what can be expected from the natural ^{13}C- and ^{15}N- containing versions of the non-protonated compound

(rather than from any non-oxidized $[M+H]^+$ ions) (figure 3.6). No sodiated or potassiated ions are seen, but there is a small peak at $[M+14]^+$, presumably resulting from methyl esterification of one of the carboxylic acids. The commercial cobalt (III) protoporphyrin internal standard exhibited nearly identical behavior, the only difference being the absence of the methyl ester peak. The $[M]^+$ ions in each case were used for MS/MS analysis. Collision-induced dissociation of each compound gave abundant fragments at *m*/*z* 564 and 505 for the mesoporphyrin complex and *m*/*z* 560 and 501 for the protoporphyrin complex, which is a difference 59 Da and 118 Da in each case. This corresponds to the sequential loss of an acetyl group from each carboxylic acid "side-chain." Each compound was quantified by reaction monitoring mass spectrometry, watching the *m*/*z* 623 → 564 and *m*/*z* 619 → 560 transitions for the mesoporphyrin and protoporphyrin complexes, respectively (figure 3.7).

Enzyme Kinetics. Experiments were undertaken to determine the K_m and V_{max} for each substrate, as well as the linear range in time of the enzyme's activity. The Michaelis-Menten enzyme kinetics parameters were determined by varying the concentrations of each substrate (while holding the other constant) over a range of 0 to 500 µM, which incorporated all previously-reported values for this enzyme, and measuring the enzyme activity in triplicate at each level. Measured activity was fitted to a non-linear least-squares model. The K_m values for cobalt (II) chloride and mesoporphyrin IX were found to be 43.0 µM and 27.4 µM, respectively (figure 3.8). Given these values, the concentrations used in the assay were 200 µM for cobalt (II) chloride and 100 µM for mesoporphyrin IX, in each case well in excess of the K_m in order to ensure enzyme saturation and reduce the possibility of inter-sample variance in enzyme velocity.

Enzyme activity as a function of incubation time was also measured in triplicate, ranging from a lack of incubation entirely up to 48 hours incubation time. The assay was found to remain linear within the first 24 hours of incubation, followed by a decrease in the slope of the curve (figure 3.9). A 20-hour incubation was chosen for the final parameters of the assay, in an effort to maximize the amount of cobalt mesoporphyrin produced while being sure to be within the linear range.

Blank correction. A significant amount of non-enzymatic incorporation of the cobalt into the mesoporphyrin was found to occur under the conditions determined to be necessary for measurable enzyme activity. Further investigation found the amount of non-enzymatic incorporation to be extremely dependent on the concentration of the two substrates (increasing by as much as 10-fold with a mere 2-fold increase in concentration), but also extremely stable at any given concentration level. Extensive lysate-free testing was done in order to firmly establish the level of non-enzymatic incorporation for the conditions chosen for the assay. Twenty assays were carried out following the exact protocol as developed, but substituting 0.9% w/v saline solution in place of the lymphocyte lysate. Complete results can be found in table 3.1. The average result was a product-to-internal standard ratio of 0.343, with an average intra-assay variation of 2.8%, and an inter-assay relative standard deviation of 8.6% (Figure 3.10). Blank-correction can and should, therefore, be applied to real assay results.

Clinical sample analysis. After determining the necessary parameters and conditions for the assay, it was applied to a group of twelve clinical blood samples. Outdated blood vials no longer necessary for medical testing were obtained from the UW clinical lab, preserved with ACD. The

lymphocytes were isolated, and the assay was performed in triplicate on each. One of the twelve showed an inter-assay variation of more than 100%, and so was discarded. The likely source of error was in the preparation of the isolated lymphocytes for the assay procedure. The remaining 11 samples had ferrochelatase activities ranging from 1.01 to 7.60 nmol/mg lysate * hr (Figure 3.11). Complete results are shown in table 3.2. The average activity was 2.8 nmol/mg lysate * hr, and the standard deviation was 1.1 nmol/mg lysate * hr. The relative standard deviation (RSD) between injections of the same assay was 3.6%, while the average inter-assay RSD, using the same enzyme source sample, was 7.4%.

3.4 – CONCLUSIONS

Tandem mass spectrometry has been shown to be an effective and efficient diagnostic tool for the quantification of ferrochelatase in lymphocytes. The use of non-natural substrates allows for ease of analysis, as well as the avoidance of any natural interferences. Due to the high specificity of tandem mass spectrometry, the assay extract can easily be combined with that from other porphyria assays, allowing for multiplexed detections from a single injection into the mass spectrometer. The tandem mass spectrometric method is less cumbersome and more specific than previous methods.

Acknowledgments. Support of this work by the NIH-NIDDK (Grant R01 DK067859) is gratefully acknowledged. We thank Dr. Martin Sadilek for technical assistance with mass spectrometric measurements.

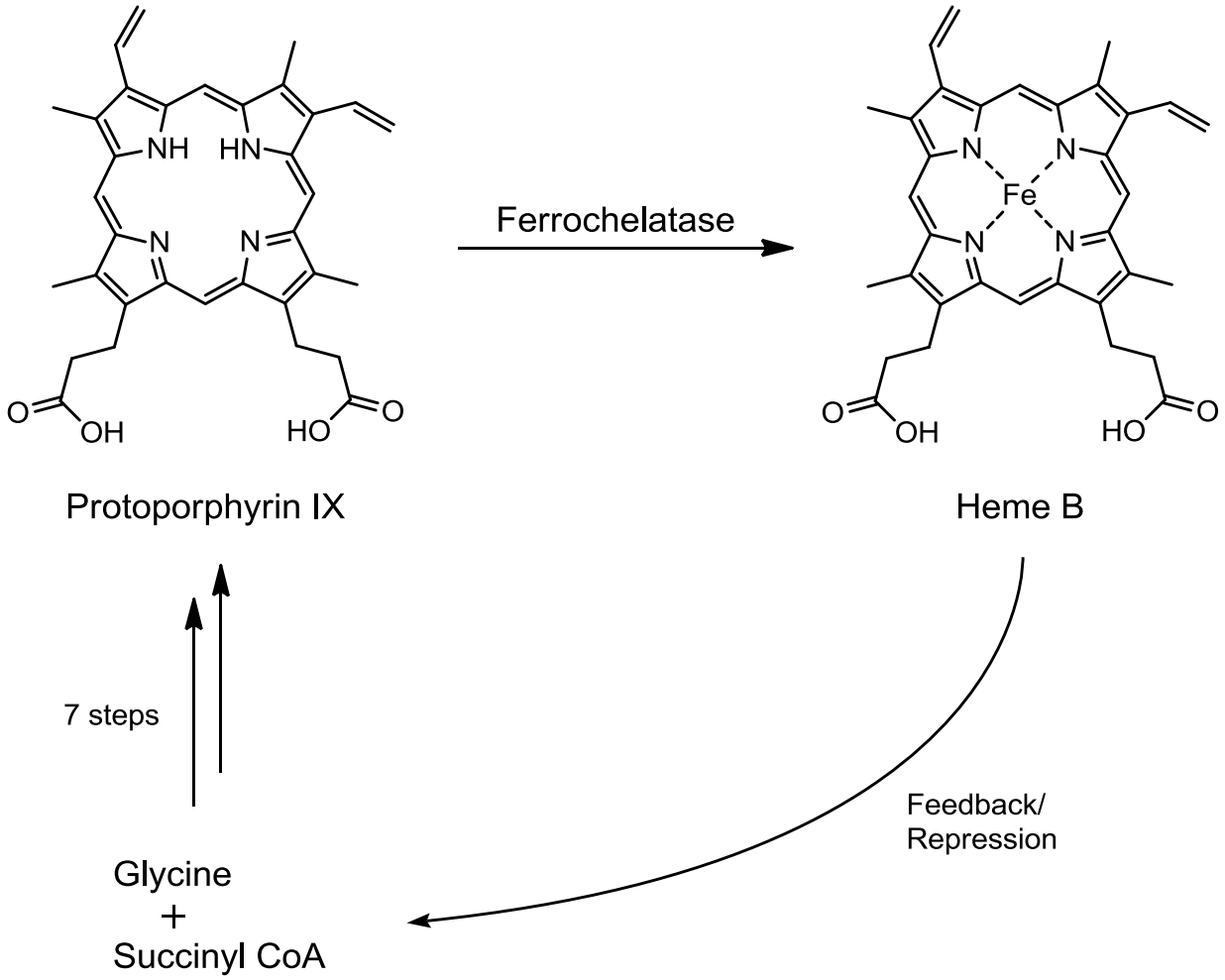

Figure 3.1. Role of ferrochelatase and heme B in the pathway.

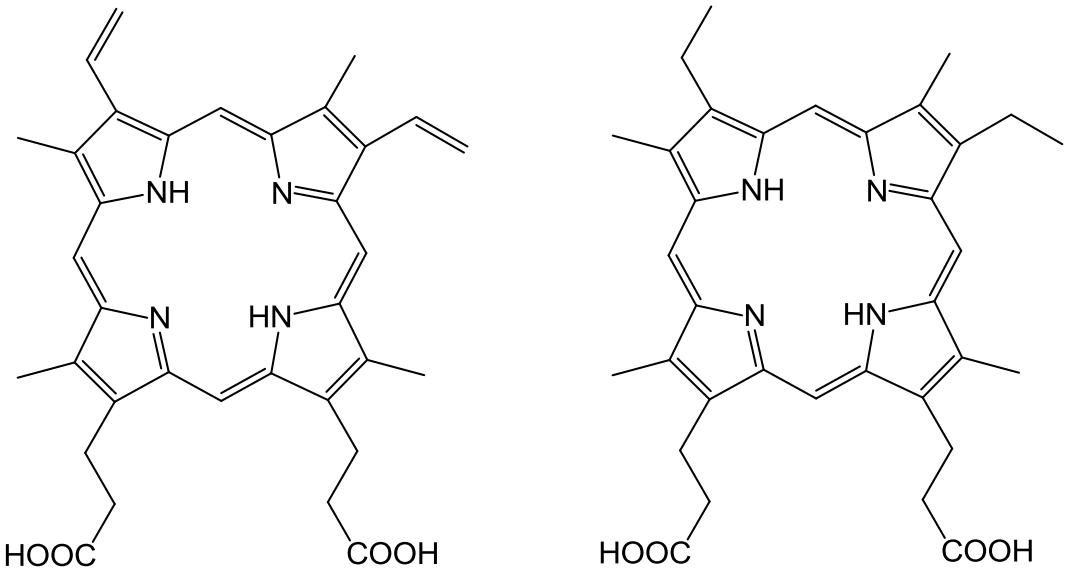

Figure 3.2. Structures of (left) protoporphyrin IX and (right) mesoporphyrin IX.

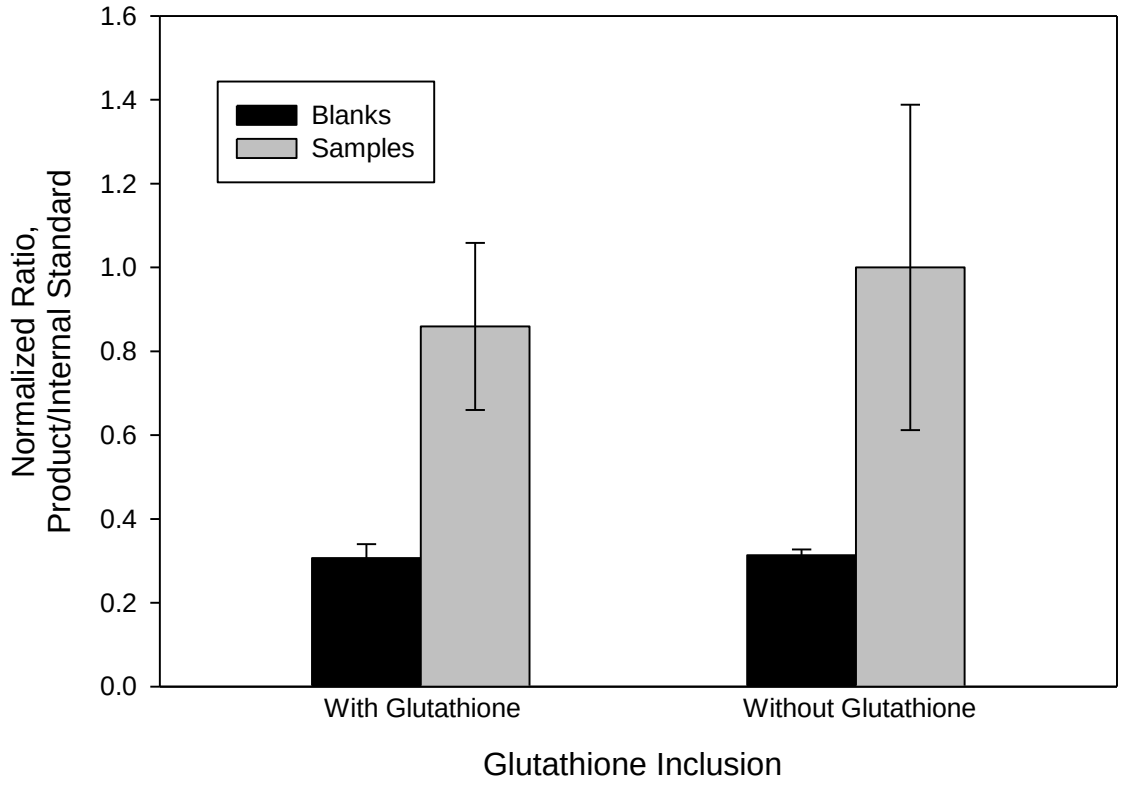

Figure 3.3. Normalized comparison of enzyme activity under standard assay conditions, with or without the inclusion of glutathione.

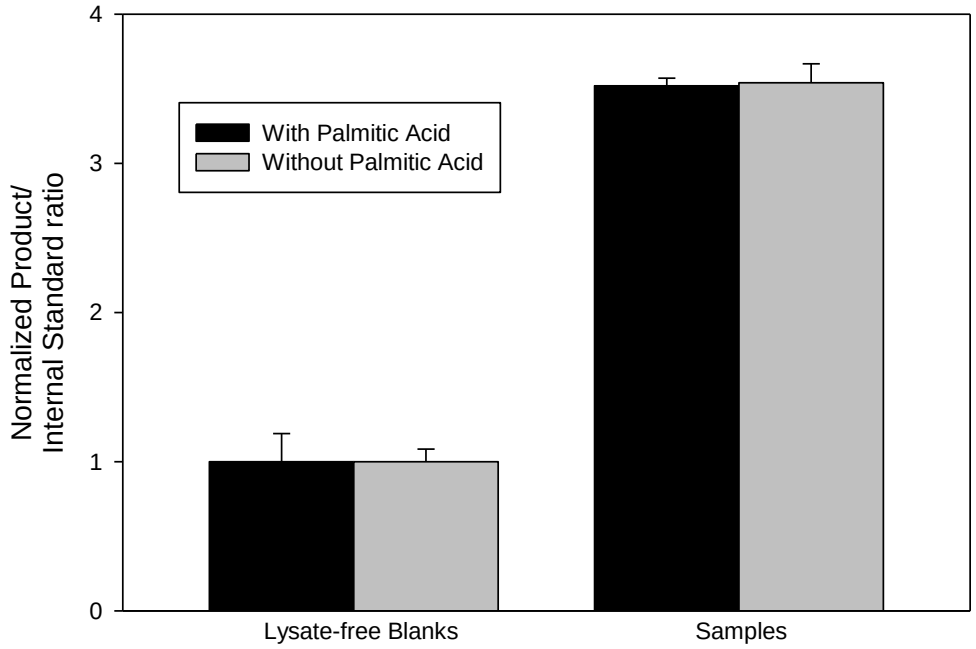

Figure 3.4. Effect of palmitic acid on measured enzyme activity. Error bars are one standard deviation based on triplicate measurements.

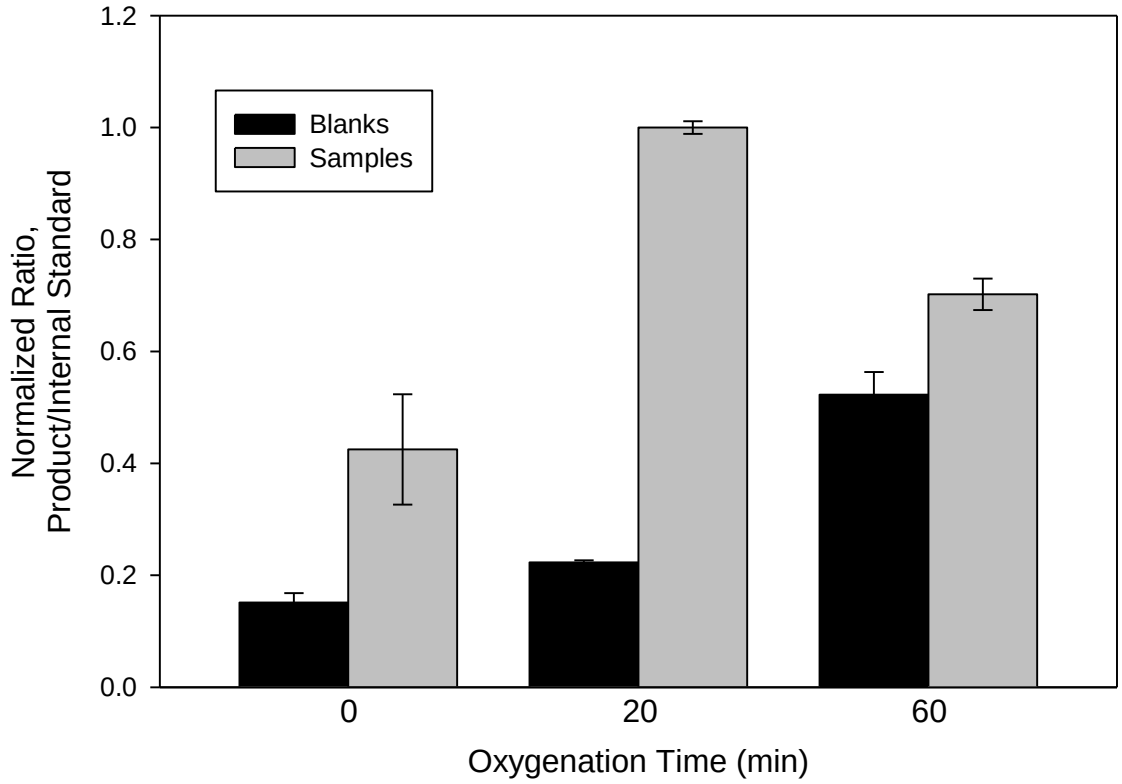

Figure 3.5. Normalized comparison of enzyme activity under standard assay conditions, varying the amount of oxidation via the bubbling of oxygen gas.

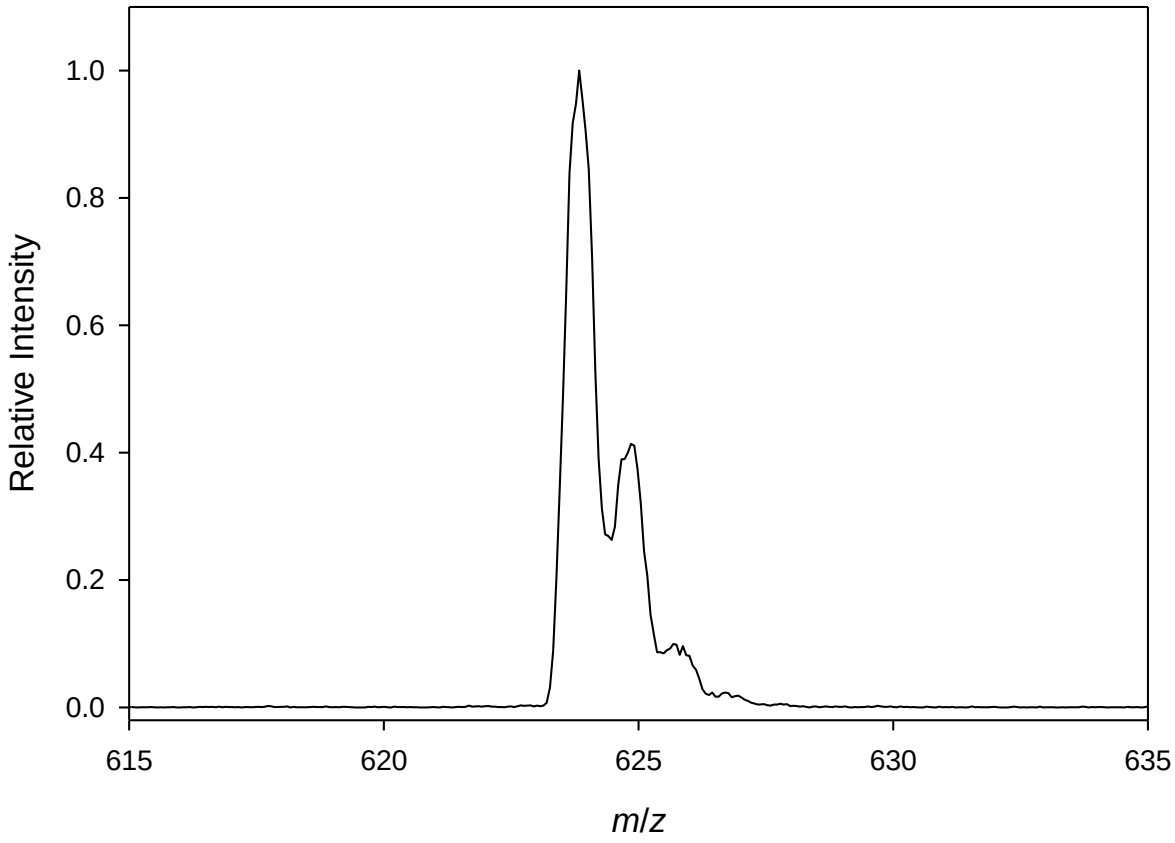

Figure 3.6. Zoomed-in mass spectrum of cobalt mesoporphyrin IX.

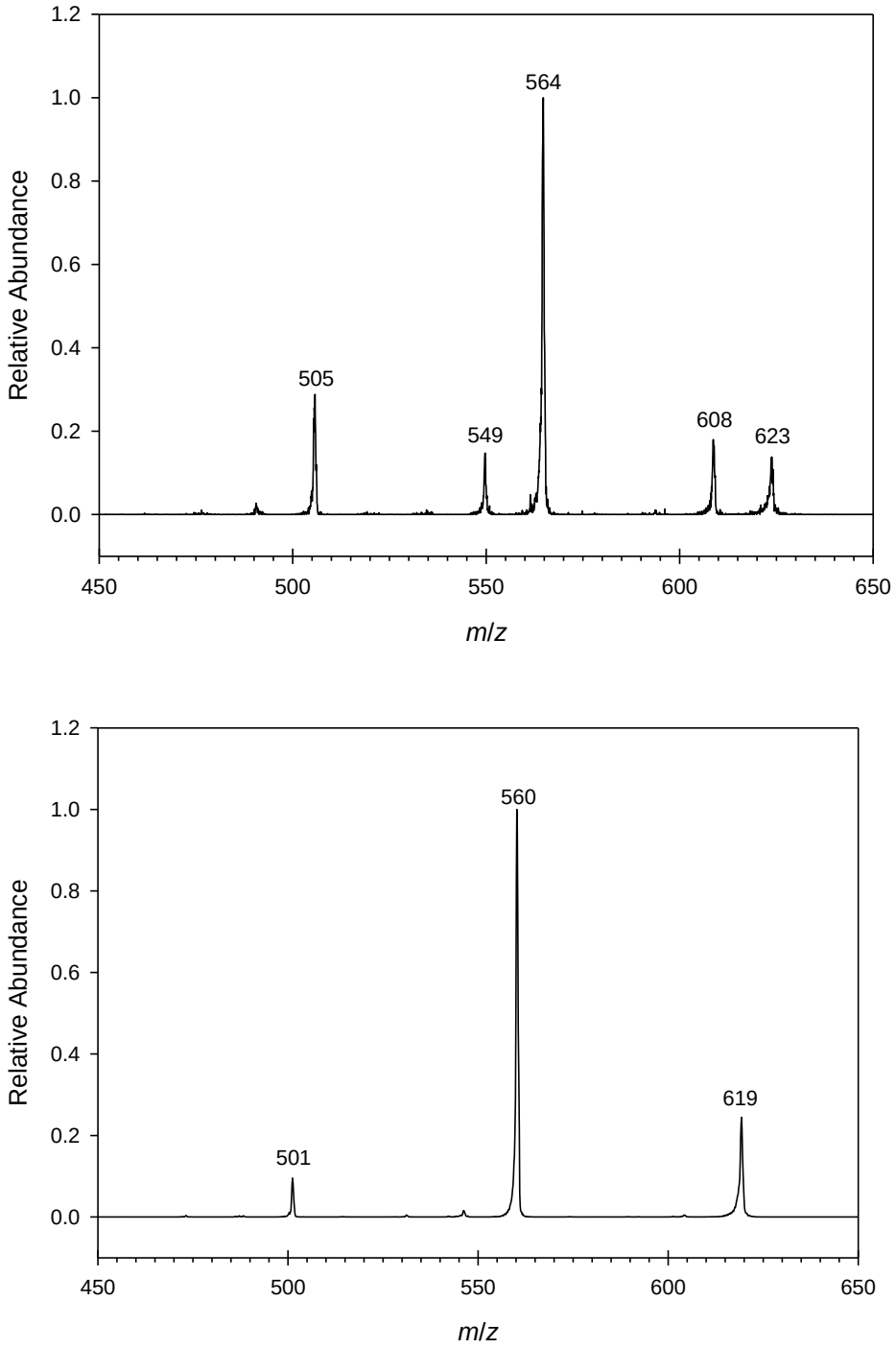

Figure 3.7. Collision-induced dissociation mass spectra at 40 eV of $[M+H]^+$ ions from (top) cobalt mesoporphyrin IX and (bottom) cobalt protoporphyrin IX.

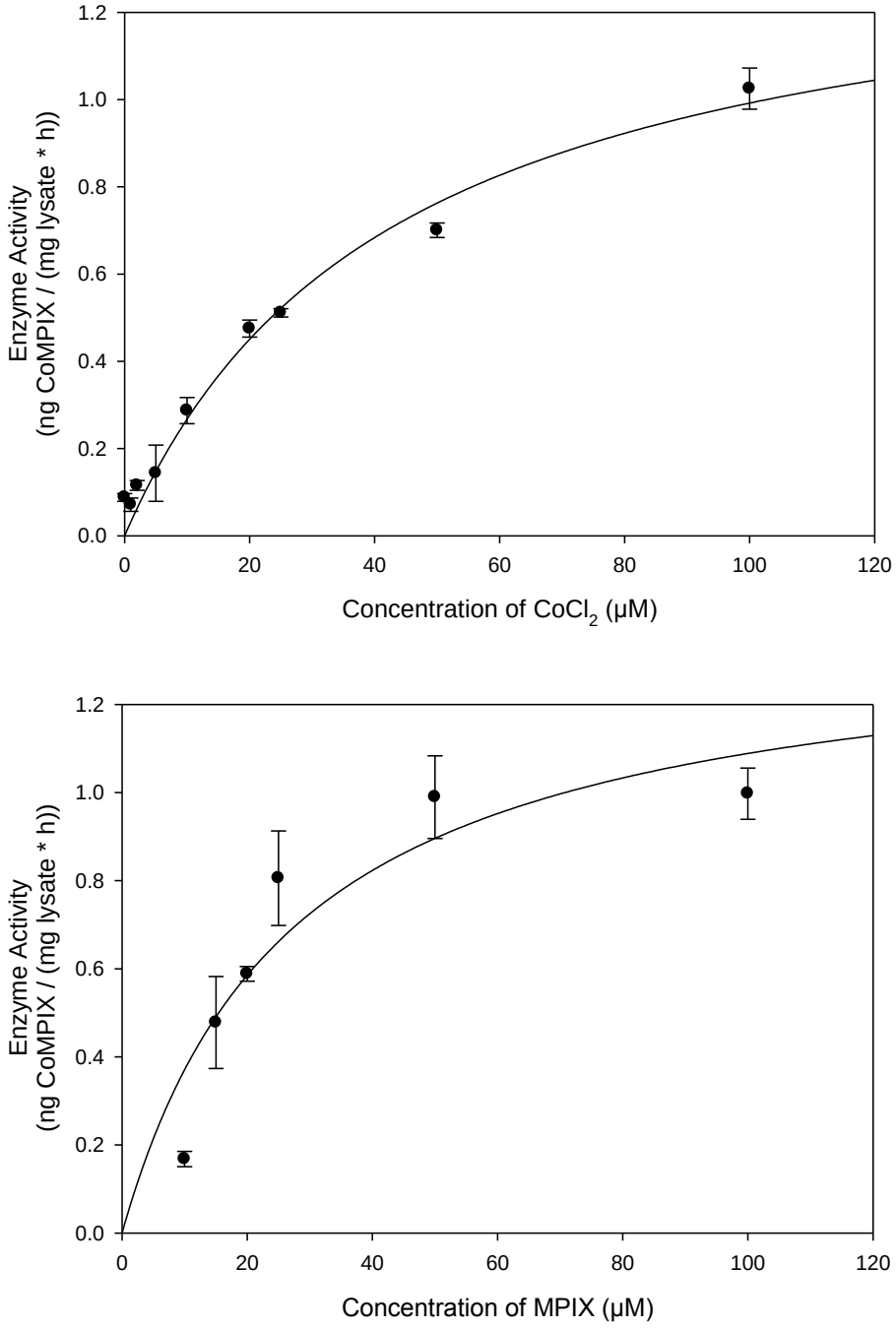

Figure 3.8. Ferrochelatase saturation curves for (top) cobalt chloride and (bottom) mesoporphyrin IX. Error bars are one standard deviation based on triplicate measurement.

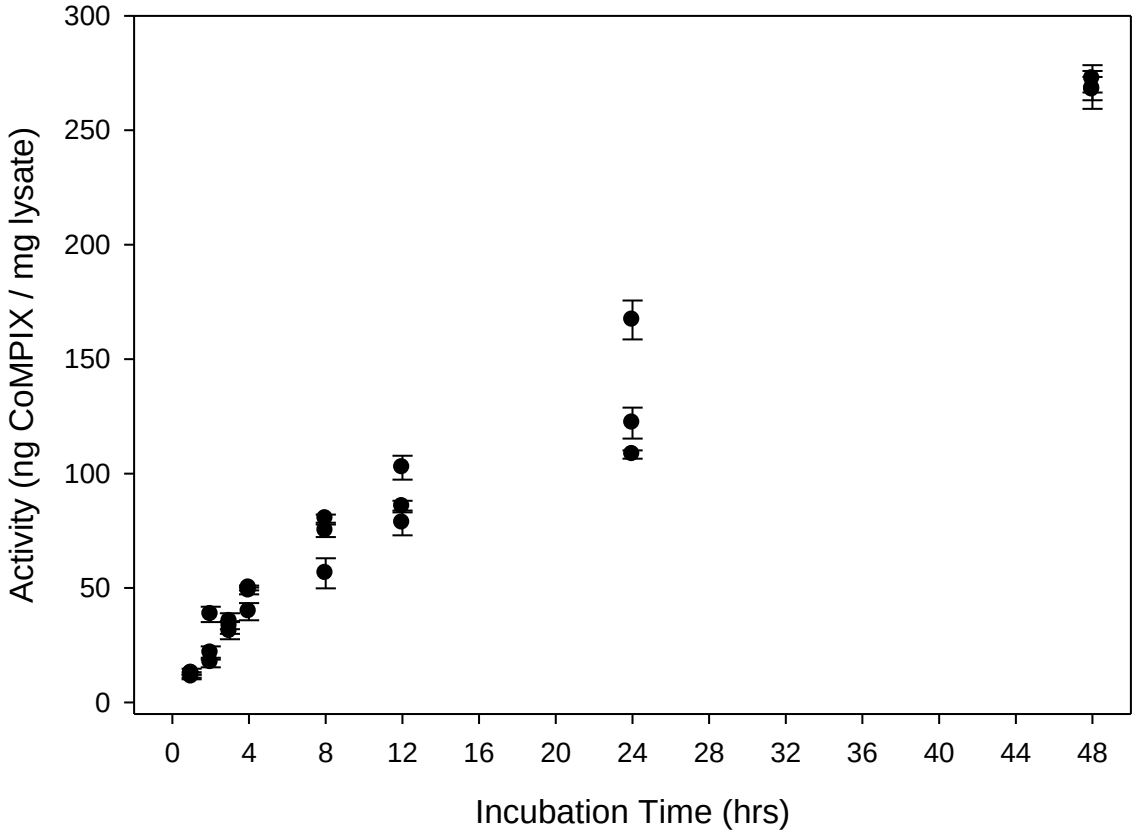

Figure 3.9. Enzyme activity versus total incubation time. Error bars are one standard deviation based on triplicate measurements.

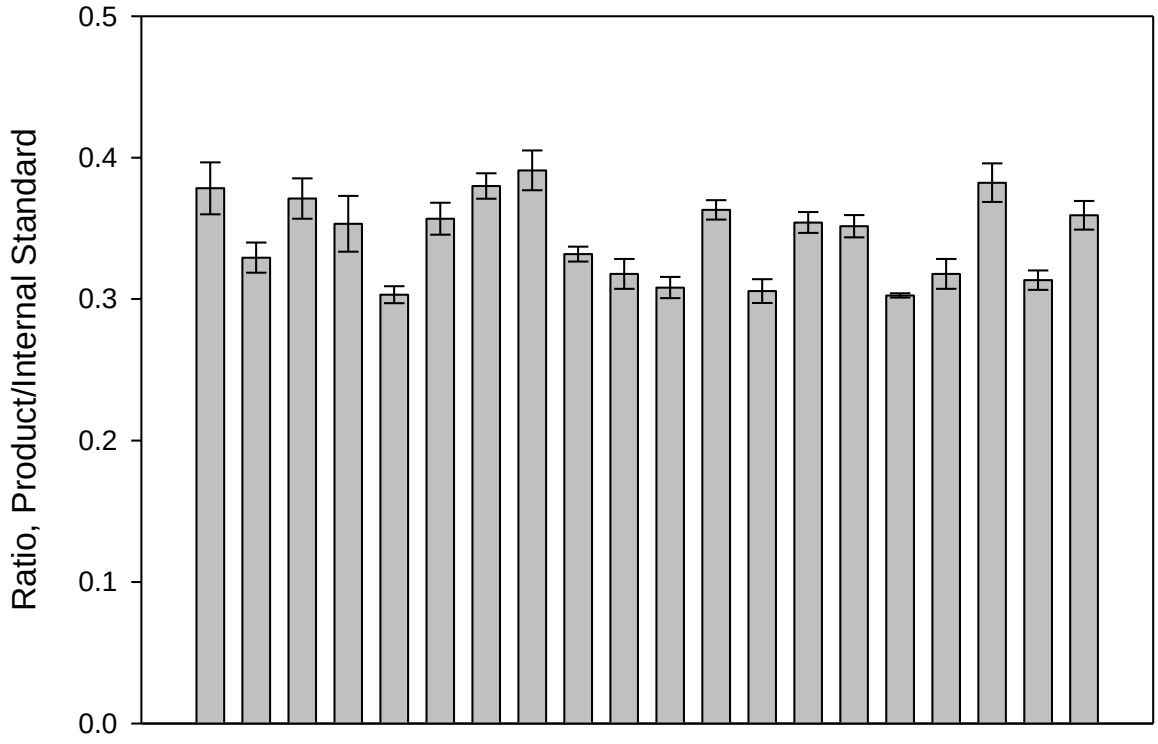

Figure 3.10. Chart of product/internal standard ratios for twenty enzyme-absent blank assays. Error bars are on standard deviation from quintuplicate measurements of each sample.

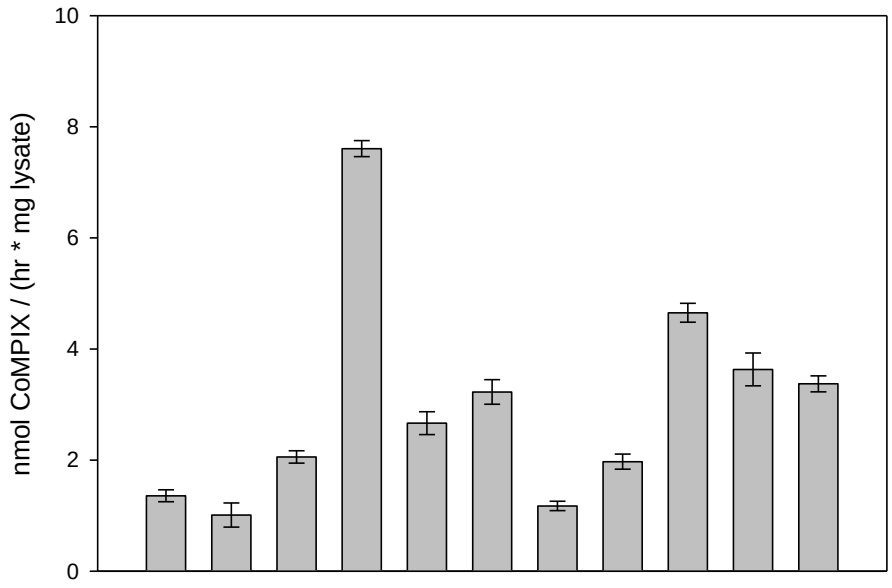

Figure 3.11. Enzyme activity from eleven random anonymous clinical lymphocyte samples. Error bars are one standard deviation from triplicate measurement of each sample.

Sample ID	Product/Internal Standard ratio	Standard Deviation
1	0.378	0.018
2	0.329	0.011
3	0.371	0.014
4	0.353	0.020
5	0.303	0.006
6	0.357	0.011
7	0.380	0.009
8	0.391	0.014
9	0.332	0.005
10	0.318	0.011
11	0.308	0.008
12	0.363	0.007
13	0.306	0.008
14	0.354	0.007
15	0.351	0.008
16	0.303	0.001
17	0.318	0.011
18	0.382	0.014
19	0.313	0.007
20	0.359	0.010

Table 3.1. Individual results from 20 lysate-free blanks. Standard deviations come from triplicate measurements.

Sample ID	Activity (nmol / h * mg lysate)	Standard deviation
1	1.36	0.11
2	1.01	0.22
3	2.05	0.11
4	7.60	0.14
5	2.67	0.21
6	3.23	0.22
7	1.17	0.09
8	1.97	0.14
9	4.65	0.17
10	3.63	0.30
11	3.37	0.14

Table 3.2. Individual results from 11 anonymous clinical samples. Standard deviations come from triplicate measurements of triplicate assays.

3.5 – REFERENCES

(1) Anderson, K.E.; Sassa, S.; Bishop, D.F.; Desnick, R.J. Disorders of Heme Biosynthesis: X-Linked Sideroblastic Anemia and the Porphyrias. In *The Metabolic and Molecular Basis of Inherited Disease*, 8th ed.; Scriver, C.R., Beaudet, A.L., Sly, W.S., Valle, D., Eds.; McGraw-Hill: New York, 2000; Chapter 124, pp 2993-2999, pp 3005-3008.

(2) Cox, T.M. *J. Inher. Metab. Dis.* **1997,** *20*, 258-269.

(3) Mathews-Roth, M.M.; Pathak, M.A.; Fitzpatrick, T.B.; Harber, L.C.; Kass, E.H. *N. Engl. J. Med.* **1970**, *282*, 1231-1234.

(4) Magnus, I.A.; Jarrett, A.; Prankerd, T.A.J.; Rimington, C. *Lancet*, **1961**, 448-451.

(5) Bloomer, J.R.; Morton, K.O. *Enzyme*, **1982**, *28*, 220-232.

(6) Wolfe, B.J.; Blanchard, S.; Sadilek, M.; Scott, C.R.; Tureček, F.; Gelb, M.H. *Anal. Chem.*, **2011,** *83* (3), 1152-1156.

(7) Spacil, Z.; Elliot, S.; Reeber, S.L.; Gelb, M.H.; Scott, C.R.; Tureček, F. *Anal. Chem.*, **2011**, *83* (12), 4822-4828.

(8) Wang, Y.; Scott, C. R.; Gelb, M.H.; Tureček, F. *Anal. Chem.*, **2008**, *80* (7), 2606-2611.

(9) Wang, Y.; Gatti, P.; Scott, C.R.; Gelb, M.H.; Tureček, F. *Anal. Chem.*, **2008**, *80* (7), 2599-2605.

(10) Choiniere, J.R.; Scott, C.R.; Gelb, M.H.; Tureček, F. *Anal. Chem.*, **2010**, *82* (15), 6730-6736.

(11) Taylor, J.F. Ph.D. Thesis, The Johns Hopkins University, Baltimore, MD, June 1940.

(12) Medlock, A.E.; Carter, M.; Dailey, T.A.; Dailey, H.A.; Lanzilotta, W.N. *J. Mol. Biol.*, **2009**, *393*, 308-319.

(13) Porra, R.J.; Ross, B.D. *Biochem. J.*, **1965**, *94*, 557-562.

(14) Rossi, R.; Costin, K.A.; Garcia-Webb, P. *Clin. Chem*, **1988**, *34*, 2481-2485.

(15) Li, F.; Lim, C.F.; Peters, T.J. *Biomed. Chromatogr.*, **1987**, *2*, 164-168.

Chapter 4.

Uroporphyrinogen III Synthase

ABSTRACT

Efforts are described towards an assay for the enzyme uroporphyrinogen III synthase, which catalyzes the rearrangement and cyclization of hydroxymethylbilane to uroporphyrinogen III. The intention of the assay development was for eventual implementation in the clinical diagnosis of cutaneous erythropoietic porphyria, a rare enzymatic deficiency of the heme biosynthetic pathway. The goal was to separate the enzymatic product, uroporphyrinogen III, from the non-enzymatically-produced isomer uroporphyrinogen I by liquid chromatography before analysis by tandem mass spectrometry. However, separation was not achieved; replication of previously reported methods did not match the reported results, and novel methods did not prove successful.

4.1 – INTRODUCTION

Heme-based compounds, such as hemoglobin, myoglobin, and the cytochrome enzymes, play a vital role in human life. The common functional group to all these, heme, is a tetrapyrrole ring-shaped molecule synthesized in the body through an eight-step, enzyme-assisted pathway. Genetic deficiency in any of the last seven of these enzymes defines the set of conditions known as the porphyrias (1). The fourth enzyme in the pathway, uroporphyrinogen III synthase

(UROS), cyclizes the linear tetrapyrrole hydroxymethylbilane after detaching, flipping, and reattaching one of the pyrroles, creating uroporphyrinogen III (figure 4.1). Deficiency in this enzyme causes the disease congenital erythropoietic porphyria (CEP). UROS is one of four heme-associated enzymes found in the cytosol of the cell.

The cyclization of hydroxymethylbilane is notable in the pathway as the only place at which significant non-enzymatic consumption of the substrate is known. While the enzyme carries out a slight rearrangement before creating the ring, thus making uroporphyrinogen III, hydroxymethylbilane rapidly and spontaneously cyclizes without the rearrangement to create the isomer uroporphyrinogen I. As such, UROS is by far the fastest enzyme in the pathway. Figure 4.2 illustrates the difference between the isomers. The non-enzymatic product is acted on by the subsequent enzyme, uroporphyrinogen decarboxylase (UROD), but only the III isomer is a substrate for the second downstream enzyme, coproporphyrinogen oxidase (CPO) (figure 4.3). Rather than leading to a buildup of the hydroxymethylbilane, then, a deficiency in UROS leads to an accumulation of the isomer of coproporphyrinogen that cannot be used by CPO. The accumulation of coproporphyrinogen I causes the disease's primary symptom, severe photosensitivity (2).

Congenital erythropoietic porphyria is inherited in an autosomal recessive pattern (3). While exceedingly rare (roughly 130 cases are known to have occurred), it was in fact the first type of porphyria to be described (4). The condition is considered to be an erythropoietic type of porphyria, which indicates that the deficiency primarily occurs in the bone marrow, rather than in the liver. Current diagnostic methods rely first on the presentation of symptoms (reddish urine in addition to the severe photosensitivity), then genetic sequencing to confirm the diagnosis. Some enzyme assays have been developed, but are not in wide use (5, 6).

Previous work in our laboratory has focused on the development of assays for determining enzyme activity levels in human samples using tandem mass spectrometry as a common analytical platform for both clinical diagnostics and newborn screening. The procedure typically involves selecting an appropriate biological enzyme source (typically blood sample lysate for clinical diagnostics and dried blood spots for newborn screening) (7-10), incubating the sample with an appropriate substrate, and quantifying the enzymatic product against a mass-differentiated internal standard by reaction-monitoring mass spectrometry. This method takes full advantage of the speed, sensitivity, and selectivity offered by mass spectrometry over slower methods. Further, the unique masses used for each assay's product and standard allows for easy multiplexed analysis, as the products of many different assays can be injected in the same sample without any need for chromatographic separation.

Previous work in the area of porphyria diagnostics has led to mass spectrometric diagnostic assays for acute intermittent porphyria, porphyria cutanea tarda, hepatoerythropoietic porphyria, hereditary coproporphyria (9, 10), δ-aminolevulinic acid dehydratase-deficient porphyria, and erythropoietic protoporphyria. This vein of research attempted to add an assay for congenital erythropoietic porphyria; however, the various attempts were not successful for reasons that will be described.

4.2 – EXPERIMENTAL

Materials. All water used was purified by a Millipore milli-q 18 MΩ filtering system. Uroporphyrin isomers I and III were purchased from Frontier Scientific (Provo, UT); all other chemicals were obtained from Sigma-Aldrich (St. Louis, MO).

Conversion of uroporphyrins to octamethyl esters. Either isomer of uroporphyrin was dissolved in excess methanol. An acid catalyst was then added, at 0.1% the volume of methanol used. Reactions were attempted with both H_2SO_4 and acetyl chloride; both were successful, but H_2SO_4 produced a more uniform product with greater speed and was the only catalyst used in reactions that went to the subsequent steps. The reaction flask was allowed to sit closed but not sealed tight at room temperature; completion was monitored by drawing 50 µL aliquots and checking for the reaction product by ion trap mass spectrometry. Excess sulfate ions were crashed from solution by bubbling anhydrous ammonia gas through the sample for approximately ten minutes. The resulting rusty-colored solid was collected on a fine-grade fritted funnel. This solid was redissolved in a 1:1 mixture of water and chloroform, dissolving the ester product in the chloroform layer and any residual salts or acids in the water layer. Three drops of 1 M HCl were added, and after vigorous mixing the chloroform layer was isolated by a separatory funnel; upon evaporation of the chloroform, a solid mass of uroporphyrin octamethyl ester remained.

Liquid chromatography. Analysis was conducted on a Varian ProStar HPLC system. Detection was done by UV-Vis spectroscopy in a 1 cm flow cell, at a wavelength of 400 nm. Separations were attempted using a Thermo-Fisher Hypersil-ODS 25 cm column, with 5-micron particles.

Mass Spectrometry. Analysis was conducted by LC/MS (10 µL injection volume) using a Waters Quattro Micro tandem quadrupole mass spectrometer in positive ion mode with a Waters 1525u dual-solvent HPLC pump system. Separation attempts were conducted using a Thermo-

Fisher Hypersil-ODS 25 cm column, with 5-micron particles. Solvents, mobile phase composition, and gradients varied depending on the specific experiment being run. The instrument was operated using MassLynx software with the following parameters: electrospray ionization capillary voltage: 4.50 kV; cone voltage: 100 V; extractor: 2 V; RF lens voltage: 100 mV; source temperature: 100° C; desolvation temperature: 350° C; desolvation gas flow: 400 L/hr; dwell time: 100 µs; collision energy: 65 eV; collision gas: argon, 1.97 mTorr.

4.3 – RESULTS AND DISCUSSION

Oxidation of relevant compounds. The compound used by the heme biosynthetic pathway is uroporphyrinogen III; however, the compound discussed in the preceding text as well as what follows is uroporphyrin III. This is because the uroporphyrinogen III, and indeed all porphyrinogen-type compounds of relevance to this pathway, rapidly oxidize in the presence of air to their respective porphyrins.

Isomer separation. The primary obstacle that must be overcome in creating an assay for UROS is the separation of uroporphyrinogens I and III. The two isomers were found to have nearly identical mass spectra and fragmentation patterns, and so the degree to which a certain fragment is present cannot be a means for quantifying the levels of each. Hence, in order to quantify the compounds by mass spectrometry, they must be separated in advance. Methods have been reported that purport to accomplish this task, with resolution at or near baseline. The most promising, in fact the only one that did not take upwards of twelve hours or require up to five reinjections of separation products onto the same column, used a mobile phase consisting of a mix of acetonitrile and 1 M acetic acid buffer, with the pH tightly controlled at 5.16. However, a

buffer of such ionic strength is incompatible with analysis by mass spectrometry. Initial experiments attempted separations using a similar system but with a more MS-friendly solvent by reducing the buffer strength to 0.1 M; unfortunately, no separation was achieved. A scheme was then devised to wash away the 1 M buffer following separation, requiring the use of an additional pump and column, which also had the side benefit of eliminating the undesired isomer without ever exposing it to the mass spectrometer. In preparation for attempting this method, experiments were undertaken to replicate the results published in the original paper; however, after repeated attempts, using multiple HPLC instruments and multiple columns (including the same model column as the original), the results were not found to be reproducible, and in fact no separation was achieved at all. Figure 4.6 shows the best spectrum collected.

Switch to octamethyl esters. After the standard forms of the two uroporphyrins proved unseparable by any reasonable measures, an effort was undertaken to attempt to separate the compounds as octamethyl esters. Mass spectra of the two compounds can be seen in figures 4.4 and 4.5. As octamethyl esters, neither compound was soluble in aqueous solvents; as such, separations using chloroform-based solvent systems were attempted, still using the same Hypersil-ODS column. Many variants on mobile phase composition and other factors were attempted, and although good chromatography was achieved, the two isomers were never able to be separated (figure 4.7).

4.4 – CONCLUSIONS

Tandem mass spectrometry, while certainly of great use in the diagnosis of many types of porphyria, has not been shown to be effective in quantifying uroporphyrinogen synthase for the

diagnosis of congenital erythropoietic porphyria. While many of the principles from earlier-developed assays for other enzymes are applicable here, the existence of a significant non-enzymatic pathway for the substrate to take proves to be too high of a hurdle here, as the separation of the enzymatic and non-enzymatic products is required but after much experimentation could not be realized.

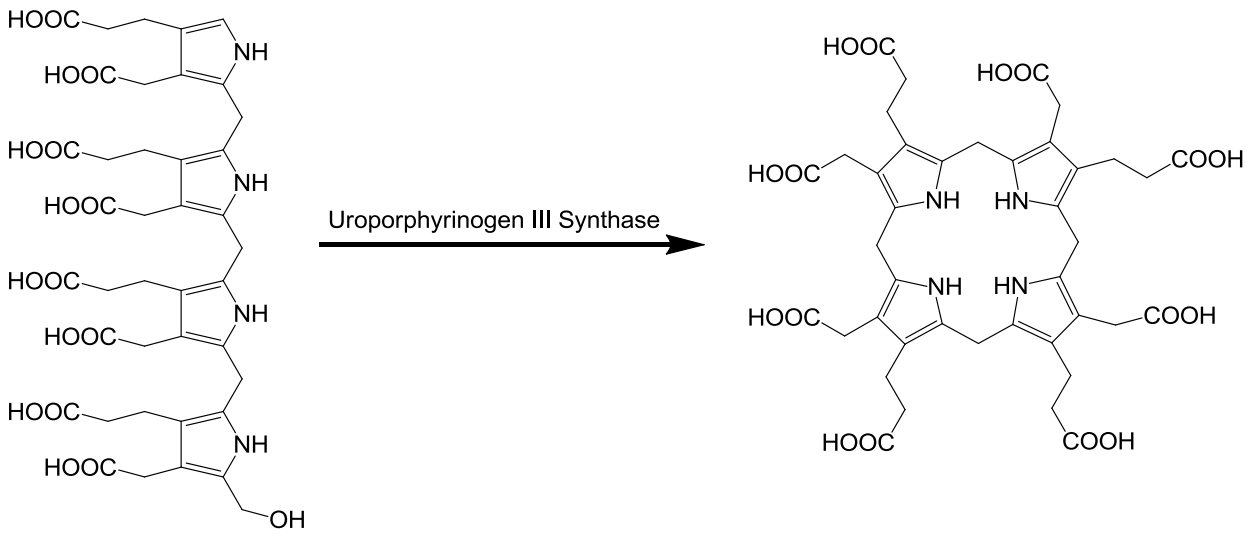

Figure 4.1. Uroporphyrinogen III synthase portion of the heme biosynthesis pathway.

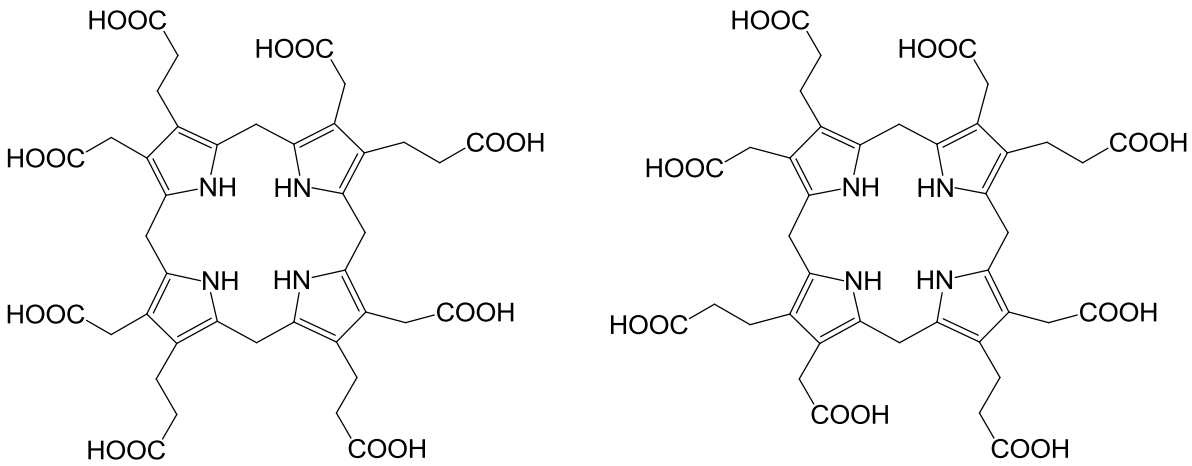

Figure 4.2. Structures of (left) uroporphyrinogen III and (right) uroporphyrinogen I.

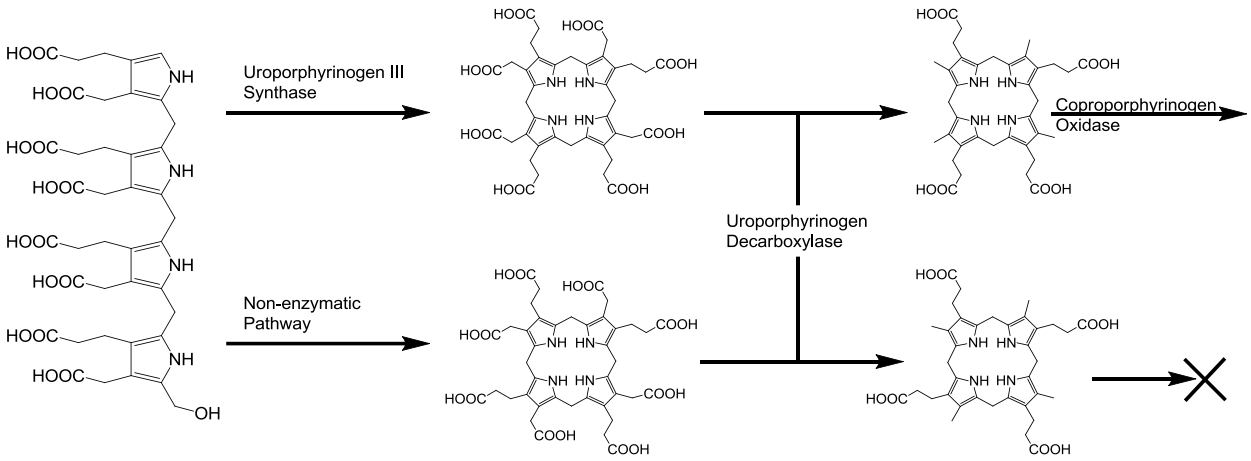

Figure 4.3. Steps 4 – 6 of the heme biosynthesis pathway. The non-enzymatic pathway stops after the decarboxylase.

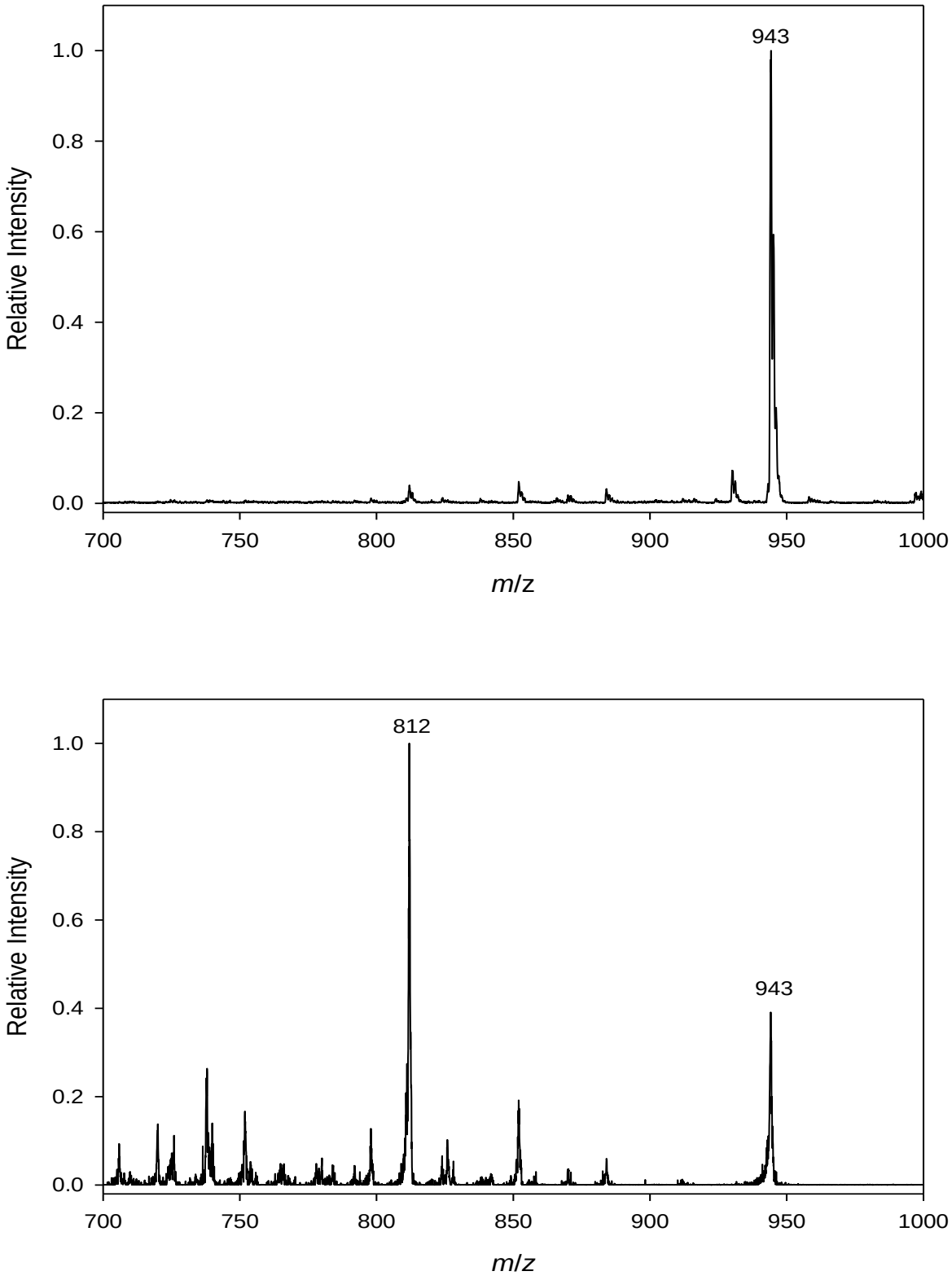

Figure 4.4. MS and MS/MS spectra of uroporphyrin I.

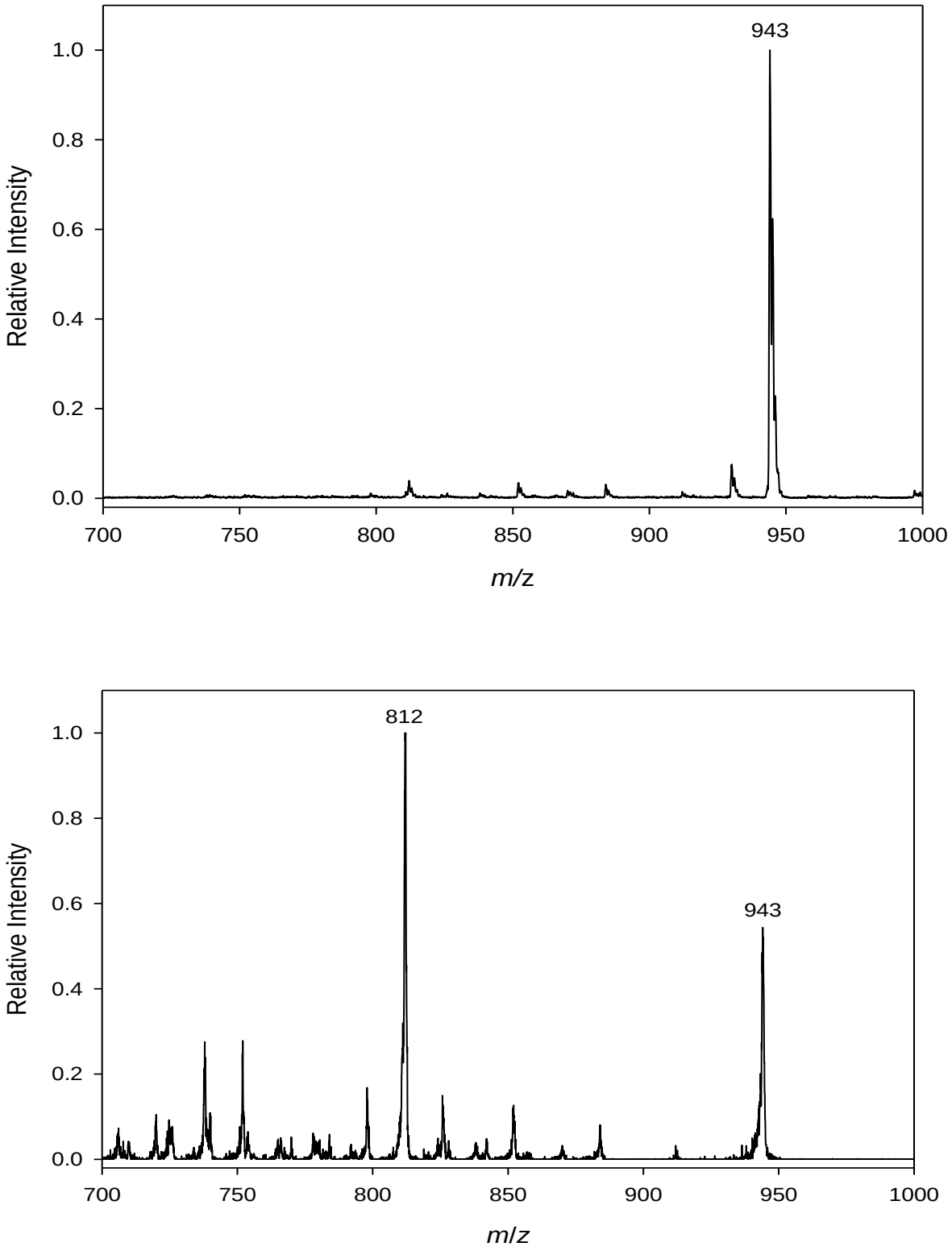

Figure 4.5. MS and MS/MS spectra of uroporphyrin III.

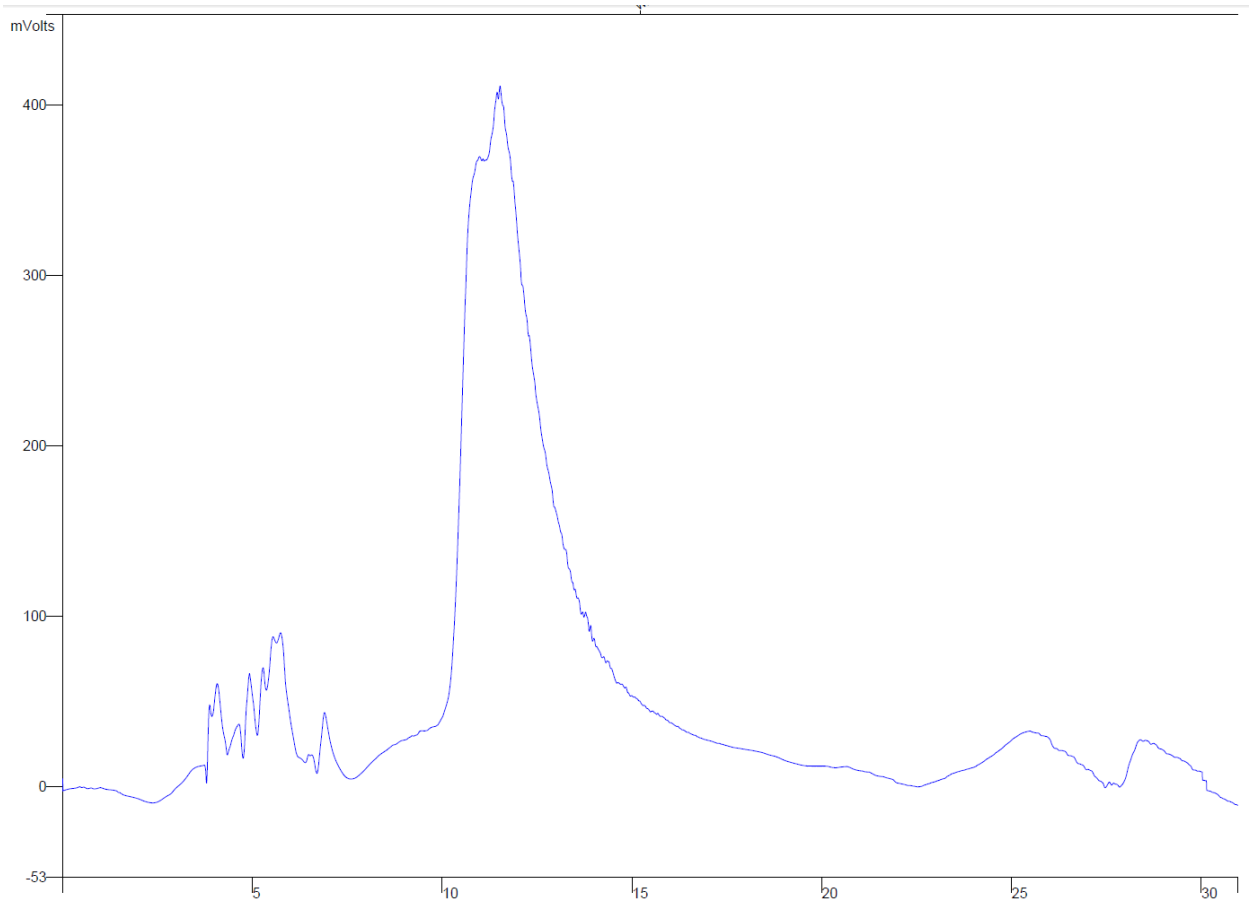

Figure 4.6. Best LC spectrum of uroporphyrin isomer mixture.

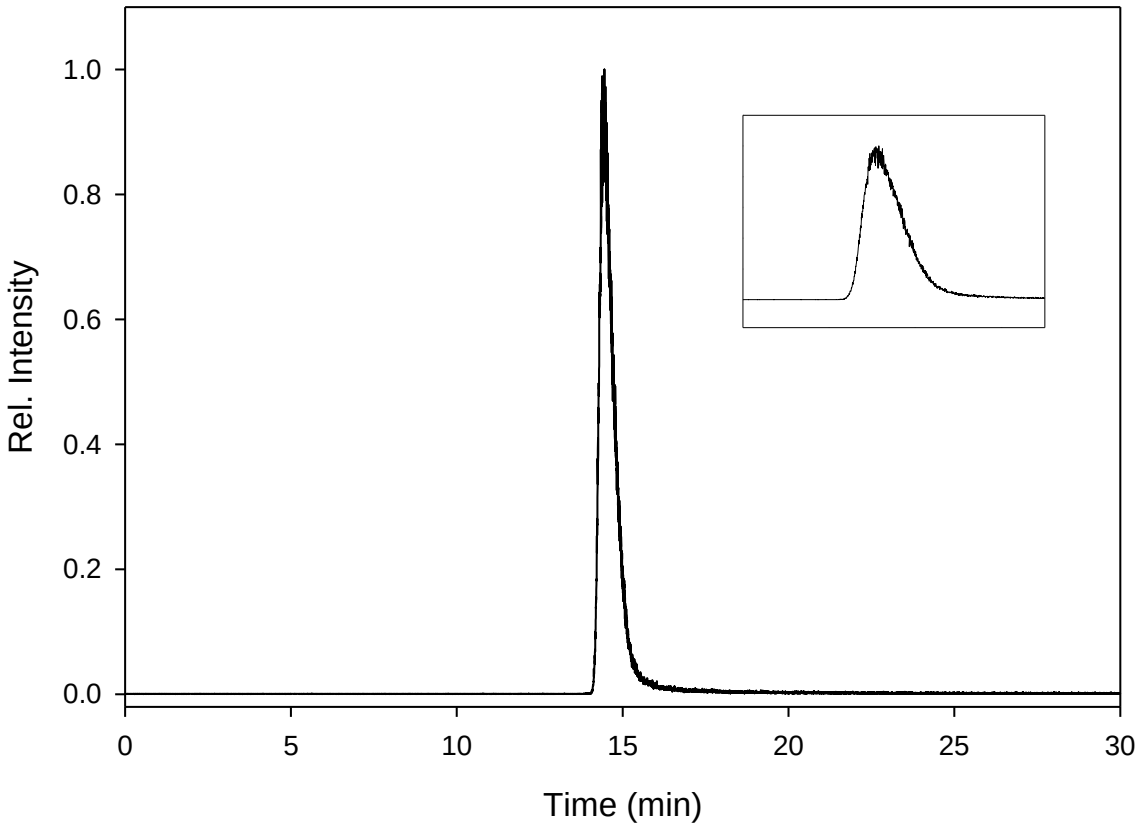

Figure 4.7. LC/MS of uroporphyrin isomer mixture. Inset is a zoomed-in view of the peak, showing no separation at all.

4.5 – REFERENCES

(1) Anderson, K.E.; Sassa, S.; Bishop, D.F.; Desnick, R.J. Disorders of Heme Biosynthesis: X-Linked Sideroblastic Anemia and the Porphyrias. In *The Metabolic and Molecular Basis of Inherited Disease*, 8th ed.; Scriver, C.R., Beaudet, A.L., Sly, W.S., Valle, D., Eds.; McGraw-Hill: New York, 2000; Chapter 124.

(2) Fritsch, C.; Bolsen, K.; Ruzicka, T.; Goerz, G. *J. Am. Acad. Dermatol.* **1997**, *36*, 594.

(3) Romeo, G.; Levin, E.Y. *Proc. Natl. Acad. Sci.* **1969**, *63*, 856.

(4) Gunther, H. *Deutsch. Archiv. Klin. Med.* **1911**, *105*, 89.

(5) Tsai, S.F.; Bishop, D.F.; Desnick, R.J. *Anal. Biochem.* **1987**, *166*, 120.

(6) Shoolingen-Jordan, P.M. *Method Enzymol.* **1997**, *281*, 327.

(7) Wolfe, B.J.; Blanchard, S.; Sadilek, M.; Scott, C.R.; Tureček, F.; Gelb, M.H. *Anal. Chem.* **2011**, *83*, 1152-1156.

(8) Duffey, T.A.; Khaliq, T.; Scott, C.R.; Tureček, F.; Gelb, M.H. *Bioorg. Med. Chem. Lett.* **2010**, *20*, 5994-5996.

(9) Wang, Y.; Gatti, P.; Sadilek, M.; Scott, C.R.; Tureček, F.; Gelb, M.H. *Anal. Chem.* **2008**, *80*, 2599-2605.

(10) Wang, Y.; Scott, C.R.; Tureček, F.; Gelb, M.H. *Anal. Chem.* **2008**, *80*, 2606-2611.

Complete Bibliography

- Akagi, R.; Kato, N.; Inoue, R.; Anderson, K. E.; Jaffe, E. K.; Sassa, S. *Mol. Genet. Metab.* ***2006****, 87 (4)*, 329-336.
- Anderson, K.E.; Sassa, S.; Bishop, D.F.; Desnick, R.J. Disorders of Heme Biosynthesis: X-Linked Sideroblastic Anemia and the Porphyrias. In The Metabolic and Molecular Basis of Inherited Disease, 8th ed.; Scriver, C.R., Beaudet, A.L., Sly, W.S., Valle, D., Eds.; McGraw-Hill: New York, 2000; Chapter 124.
- Anderson, P.M.; Desnick, R.J. *J. Biol. Chem.* **1979**, *254*, 6924-6930.
- Bird, T.D.; Hamernyik, P.; Nutter, J.Y.; Labbe, R.F. *Am. J. Hum. Genet*. **1979**, *31*, 662-668.
- Bishop, D.F.; Desnick, R.J. *Method Enzymol*. **1986**, *123*, 339-345.
- Blanchard, S.; Sadilek, M.; Scott, C.R.; Tureček, F.; Gelb, M.H. *Clin. Chem*. **2008**, *54*, 2067-2070.
- Bloomer, J.R.; Morton, K.O. *Enzyme*, **1982**, *28*, 220-232.
- Caggana, M; Saavedra, C.; Wenger, D.; Helton, L.; Orsini, J. *Mol. Genet. Metab*. **2008**, *93*, S17.
- Cameron, A.E.; Eggers, D.F. *Rev. Sci. Instrum*. **1948**, *19*, 605.
- Chang, C. S.; Sassa, S. *Blood* **1985**, *65*, 939-944.
- Choiniere, J.R.; Scott, C.R.; Gelb, M.H.; Tureček, F. *Anal. Chem*. **2010**, *82 (15)*, 6730-6736.
- Comisarow, M.B.; Marshall, A.G. *Chem. Phys. Lett*. **1974**, *25*, 282.
- Cox, T.M. *J. Inher. Metab. Dis*. **1997**, *20*, 258-269.
- Doss, M.; Sassa, S. The Porphyrias. In Laboratory Medicine. The Selection and Interpretation of Clinical Laboratory Studies; Noe, D.A., Rock, R.C., Eds.; Williams and Wilkins: Baltimore, MD, 1994; Chapter 26, pp 535-553.
- Doss, M.; von Tiepermann, R.; Schneider, J.; Schmid, H. *Klin. Wochenschr*. **1979**, *57*, 1123-1127.

- Duffey, T.A.; Bellamy, G.; Elliott, S.; Fox, A.C.; Glass, M.; Tureček, F.; Gelb, M.H.; Scott, C.R. *Clin. Chem.* **2010**, *56*, 1854-1861.
- Duffey, T.A.; Khaliq, T.; Scott, C.R.; Tureček, F.; Gelb, M.H. *Bioorg. Med. Chem. Lett*. **2010**, *20*, 5994-5996.
- Duffner, P.K.; Caggana, M.; Orsini, J.; Wenger, D.A.; Patterson, M.C.; Crosley, C.J.; Kurtzberg, J.; Arnold, G.L.; Escolar, M.L.; Adams, D.J.; Andriola, M.R.; Aron, A.M.; Ciafaloni, E.; Djukic, A.; Erbe, R.W.; Galvin-Parton, P.; Helton, L.E.; Kolodny, E.H.; Kosofsky, B.E.; Kronn, D.F.; Kwon, J.M.; Levy, P.A.; Miller-Horn, J.; Naidich, T.P.; Pellegrino, J.E.; Provenzale, J.M.; Rothman, S.J.; Wasserstein, M.P. *Pediatr. Neurol.* **2009**, *40*, 245-254.
- Elder, G.; Harper, P.; Badminton, M.; Sandber, S.; Deybach, J.-C. *J. Inherit. Metab. Dis*. [Online early access]. DOI: 10.1007/s10545-012-9544-4. Published Online: 11/1/2012.
- Fenn. J.B.; Mann, M.; Meng, C.K.; Wong, S.F.; Whitehouse, C.M. *Science*, **1989**, *246*, 64-71.
- Fritsch, C.; Bolsen, K.; Ruzicka, T.; Goerz, G. *J. Am. Acad. Dermatol.* **1997**, *36*, 594.
- Furuyama, K.; HArigae, H.; Kinoshita, C.; Shimada, T.; Miyaoka, K.; Kanda, C.; Maruyama, Y.; Shibahara, S.; Sassa, S. *Blood* **2003**, *101*, 4623-4624.
- Gelb, M. H.; Tureček, F.; Scott, C. R.; Chamoles, N. A. *J. Inherited Metab. Dis*. **2006**, *29*, 397-404.
- Gerber, S.A.; Scott, C.R.; Tureček, F.; Gelb, M.H. *Anal. Chem*. **2001**, *73*, 1651-1657.
- Gerber, S.A.; Scott, C.R.; Tureček, F.; Gelb, M.H. *Bioconjugate Chem*. **2001**, *12*, 603-615.
- Gerber, S.A.; Scott, C.R.; Tureček, F.; Gelb, M.H. J. *Am. Chem. Soc*. **1999**, *121*, 1102-1103.
- Giampetro, P.F.; Desnick, R.J. *Anal. Biochem*. **1983**, *131*, 83-92.
- Gross, U.; Hoffman, G.F.; Doss, M.O. *J. Inherit. Metab. Dis*. **2000**, *23 (7)*, 641-661.
- Gunther, H. Deutsch. *Archiv. Klin. Med*. **1911**, *105*, 89.
- Hederstedt, L.; Lewin, A.; Throne-Holst, M. *J. Bacteriol*. **2005**, *187*, 8361-8369.
- Hu, Q.; Noll, R.J.; Li, H.; Makarov, A.; Hardman, M.; Cooks, R.G. *J. Mass Spectrom*. **2005**, *40 (4)*, 430-443.

- Khaliq, T.; Sadilek, M.; Scott, C.R.; Tureček, F.; Gelb, M.H. *Clin. Chem*. **2011**, *57*, 128-131.
- Li, Y.; Brockmann, K.; Tureček, F.; Scott, C.R.; Gelb, M.H. *Clin. Chem*. **2004**, *50*, 638-640.
- Lüönd, R.M.; Walker, J.; Neier, R.W. *J. Org. Chem*. **1992**, *57*, 5005-5013.
- Magnus, I.A.; Jarrett, A.; Prankerd, T.A.J.; Rimington, C. *Lancet*, **1961**, 448-451.
- Mathews-Roth, M.M.; Pathak, M.A.; Fitzpatrick, T.B.; Harber, L.C.; Kass, E.H. *N. Engl. J. Med.* **1970**, *282*, 1231-1234.
- Mauzerall, D.; Granick, S. *J. Biol. Chem*. **1955**, *219*, 435-446.
- Medlock, A.E.; Carter, M.; Dailey, T.A.; Dailey, H.A.; Lanzilotta, W.N. *J. Mol. Biol.* **2009**, *393*, 308-319.
- Miller, P.E.; Denton, M.B. *J. Chem. Ed*. **1986**, *63*, 617-622.
- Orsini, J.; Morrissey, M.A.; Slavin, L.N.; Wojcik, M.l Biski, C.; Martin, M.; Keutzer, J.; Zhang, X.K.; Chuang, W.L.; Elbin, C.; Caggana, M. *Clin. Biochem*. **2009**, *42*, 877-884.
- Paul, W. U.S. Patent 2,939,952, 1960.
- Paul, W.; Steinwedel, H.Z. *Naturforsch A*, **1953**, *8*, 448.
- Porra, R.J.; Ross, B.D. *Biochem. J*., **1965**, *94*, 557-562.
- Romeo, G.; Levin, E.Y. *Proc. Natl. Acad. Sci*. **1969**, *63*, 856.
- Sassa, S. *Enzyme* **1982**, *28*, 133-145.
- Sassa, S.; Fujita, H.; Kappas, A. *Pediatrics*, **1990**, *86*, 84-86.
- Sassa, S.; Granick, S.; Kappas, A. *Ann. NY Acad. Sci*. **1975**, *244*, 419-439.
- Shoolingen-Jordan, P.M. *Method Enzymol*. **1997**, *281*, 327.
- Sleno, L.; Volmer, D.A. *J. Mass Spectrom*. **2004**, *39*, 1091-1112.
- Spacil, Z.; Elliot, S.; Reeber, S.L.; Gelb, M.H.; Scott, C.R.; Tureček, F. *Anal. Chem*, **2011**, *83 (12)*, 4822-4828.
- Taylor, J.F. Ph.D. Thesis, The Johns Hopkins University, Baltimore, MD, June 1940.
- Thompson, J.J. *Philosophical Magazine A* **1912**, *24*, 209.

- Tsai, S.F.; Bishop, D.F.; Desnick, R.J. *Anal. Biochem*. **1987**, *166*, 120.
- Wang, D.; Eadala, L.; Sadilek, M.; Chamoles, N.A.; Tureček, F.; Scott, C.R.; Gelb, M.H. *Clin. Chem*. **2005**, *51*, 898-900.
- Wang, D.; Wood, T.; Sadilek, M.; Tureček, F.; Scott, C.R.; Gelb, M.H. *Clin. Chem.* **2007**, *53*, 137-140.
- Wang, N.; Zhao, X.; Lu, Y.; *J. Am. Chem. Soc.* **2005**, *127 (47)*, 16541-16547.
- Wang, Y.; Gatti, P.; Sadilek, M.; Scott, C. R.; Tureček, F.; Gelb, M. H. *Anal. Chem*. **2008**, *80*, 2599-2605.
- Wang, Y.; Scott, C. R.; Gelb, M. H.; Tureček, F. *Anal. Chem*. **2008**, *80*, 2606-2611.
- Wigfield, D.C.; Farant, J.-P. *Clin. Chem*. **1981**, *27*, 100-103.
- Wigfield, D.C.; Farant, J.-P.; Goldberg, C.; MacKeen, J.E. *J. Anal. Tox*. **1981**, *5*, 57-61.
- Wolfe, B.J.; Blanchard, S.; Sadilek, M.; Scott, C.R.; Tureček, F.; Gelb, M.H. *Anal. Chem.* **2011**, *83*, 1152-1156.
- Wolfe, B.J.; Ghomashchi, F.; Kim, T.; Adam, C.A.; Sadilek, M.; Jack, R.; Thompson, J.N.; Scott, C.R.; Gelb, M.H.; Tureček, F. *Bioconjugate Chem*. **2012**, *23*, 557-564.
- Zhou, X.F.; Tureček, F.; Scott, C.R.; Gelb, M.H. *Clin. Chem*. **2001**, *47*, 874-881.